DETERMINATION OF THE LONGITUDINAL MAGNETIZATION CURVES OF POLARIZED NICKEL-IRON WIRES UNDER TORSIONAL STRESS

by

DWIGHT DANIEL BORNEMEIER

B. A., North Central College, 1956

A THESIS

submitted in partial fulfillment of the

requirements for the degree

MASTER OF SCIENCE

Department of Physics

KANSAS STATE UNIVERSITY
OF AGRICULTURE AND APPLIED SCIENCE

1960

PREFACE

The circular and longitudinal magnetization of nickel-iron wires under tensional and torsional stress has been measured by G. J. van der Maas (10). He used the search coil-ballistic galvanometer method to measure the longitudinal magnetization, and utilized the first Inverse Wiedemann Effect to measure the circular magnetization. Under the action of a periodic alternating magnetic field the wire changes its magnetization periodically. For wires under external stress the major portion of this change takes place discontinuously at some distinct value of the applied field. The experimental results obtained indicate that in the region $2 \leqq H \leqq 8$ oersteds, the circular and longitudinal magnetization increases with torsional stress. It was also shown that these results were independent of the waveform of the applied magnetic field over the range of audio frequencies.

Theoretical investigation of this problem under the assumptions that (a) the magnetocrystalline anisotropy energy is constant or small in comparison with the magnetoelastic and field energies, (b) the change in magnetization takes place quasi-statically, (c) internal stress is negligible, yields the result that with increasing torque the circular component of magnetization should increase and the longitudinal component should decrease for all positive values of longitudinal stress, provided that the wire has a positive linear magnetostriction coefficient. Subsequent investigations by the writer have indicated that for fields above 8.82 oersteds, increasing torque

will result in decreasing longitudinal magnetization.

It is the purpose of this research to study the magneto-mechanical processes in torqued ferromagnetic wires in the reversible region of magnetization $H \cong 0$. Thus are avoided the complications which arise from the discontinuous changes in magnetization, characteristic of the irreversible region $-\infty \leqq H \leqq \infty$. This thesis will primarily describe attempts to verify experimentally the theoretical expression given by G. J. van der Maas for the longitudinal magnetization curves of a polarized wire under torsional stress only. A. E. Asch is carrying out complementary investigations on the circular component, the results of which are to be reported in his Master's thesis.

The investigations reported here are preparatory to further investigations of the mechanisms of magnetization in stressed ferromagnetics. Therefore the conclusions and results which summarize a portion of these initial investigations are necessarily not complete.

TABLE OF CONTENTS

INTRODUCTION

For many years it has been known that a relationship exists between the stress condition and the magnetization of a ferromagnetic material. As early as 1862 Wiedemann (2) demonstrated that under the combined action of a longitudinal and circular magnetic field a ferromagnetic rod experiences a torque. This effect is known as the Wiedemann Effect. There are two inverses of the Wiedemann Effect. (a) Longitudinal magnetization of a torqued ferromagnetic rod causes circular magnetization, or torsion of a longitudinally magnetized rod causes circular magnetization. In reversing the longitudinal field this circular magnetization can be demonstrated as an emf across the wires in the direction of the longitudinal field. (b) Torsion in a circularly magnetized ferromagnetic rod causes longitudinal magnetization, or circular magnetization of a torqued rod causes longitudinal magnetization. This effect can also be demonstrated by reversing the circular magnetization (the current through the rod). The changes in the longitudinal magnetization can be observed by using a search coil whose axis lies along the direction of the axis of the rod.

A more general stress-magnetization relationship was first discovered by Joule in 1847 (6). He found that when a ferromagnetic material undergoes magnetization, the physical dimensions of the body change. This is generally referred to as magnetostriction, and is somewhat analogous to electrostriction. A material is said to have a positive linear coefficient of

magnetostriction when its length increases in the direction of the applied field upon magnetization. It is said to have a negative linear coefficient of magnetostriction when it contracts in the direction of the applied magnetic field.

More recently Sixtus and Tonks (8), Dijkstra and Snoek (5), Stewart (9), and others, have investigated the flux reversals in wires under tension. They have been primarily concerned with the speed of flux reversal as a function of the tension and the applied field.

The Phenomenological Theory of Magnetization

General Aspects. In 1907 Weiss introduced the concept of the magnetic "molecular field" in order to explain the salient features of ferromagnetism. His initial postulates now have a firm theoretical and experimental basis in the modern phenomenological and quantum mechanical theories of magnetism. The basic problem of ferromagnetism is the explanation of how very large magnetic induction values are produced by relatively small applied magnetic fields. Weiss explained ferromagnetism in terms of magnetic dipoles by postulating the existence of a "molecular field" which tended to align the individual magnetic dipoles in one direction. Their alignment thus explained the large magnetization values associated with ferromagnetic media. The principle may be seen from the simple couple on a magnetic dipole in a uniform magnetic field. Weiss recognized that the classical magnetic interaction between dipoles is much too weak to account

for the high value of the molecular field. It is now known that this field is of quantum mechanical origin. To explain the non-magnetized condition of a ferromagnetic Weiss assumed small regions called "domains" within which the local magnetization vector has a constant value. If these domains are oriented in a random manner, the total magnetization will be zero.

Becker (2) suggested that the increase in magnetization under the influence of an applied field may take place in two independent ways:

1. By growth of favorably oriented domains at the expense of unfavorably oriented domains.

2. By rotation of the domains.

The first process occurs for smaller field values than the second. The theoretical explanation of the origin of domains in terms of magnetic field energy was given by Landau and Lifshitz (7), and the physical existence of domains was first shown by Bitter (3). Williams, Bozorth, and Shockly (12) have recently shown that the domain shapes and sizes in several ferromagnetic materials under mechanical stress and magnetic forces are in good agreement with current theory due to Neel, and others. In general, the size of domains varies from 10^{-6} to 10^{-2} cm^3.

The Minimization of the Total Free Energy Expression. There are several energy terms in the total free energy expression connected with the magnetization process, but the physical shape of the test material and the range of the applied field used in this work are such that it is possible to neglect two of these terms. They are the exchange energy E_{ex}, and the magnetic self

energy E_{self}. The total energy density of magnetization is then given by $E_t = E_k + E_h + E_\sigma$, where E_k is the magnetocrystalline anisotropy energy, E_σ is the magnetoelastic energy, and E_h is the field energy. In each of these expressions the saturation magnetization vector I_s of a domain is related to some defined direction in the material. In the case of E_h the direction is that of the applied field H. For E_σ it is one of the directions of principal compressive or tensile stress, and for E_k the defined directions are the crystalographic axes of the crystal. Now if E_t is expressed in terms of an angle variable, say θ, and minimized, the resulting expression is an equation relating I_s, H, and θ. The component of I_s in a direction θ from H is related to I_s and θ through the relation $I_i = I_s \cos \theta$. Hence there are two equations, $I = I(\theta)$ and $H = H(\theta)$, representing the magnetization curves. In general, it is desirable to leave the relation in this parametric form since eliminating θ to obtain I as an explicit function of H may eliminate the multivalued property of the relationship. It has been pointed out by G. J. van der Maas (11) that minimization of either the energy density, or the total energy, results in the same relations between I and H, that is, the same equations of magnetization.

The Terms in the Free Energy Expression

The Magnetocrystalline Anisotropy Energy. In general, the magnetization is not in the same direction as the applied field.

If, however, the field is applied along an axis of symmetry in the crystal (in iron 100, 110, 111), then the magnetization has the same direction as the field. The experimental magnetization curves for single crystals with very small amounts of impurities and internal stresses reveal the existence of preferred directions of magnetization.

Akulov (1) suggested that the effect of magnetocrystalline forces could be represented by a magnetocrystalline energy term in the free energy expression for the crystal. This energy would be dependent on the direction of the domain magnetization relative to the crystal lattice. He expressed this energy as being proportional to a series of ascending powers in α_1, α_2, and α_3, the direction cosines of the magnetization relative to the principal axes of the crystal. For certain crystals the symmetry conditions cause some of the terms to drop out, since physically it is known that the final energy expression must be independent of the change of sign of any of the α or to the interchange of any two of them. Under these conditions the magnetocrystalline energy E_k for a cubic crystal is,

$$E_k = K_o + K_1(\alpha_1^2\alpha_2^2 + \alpha_2^2\alpha_3^2 + \alpha_3^2\alpha_1^2) + K_2(\alpha_1^2\alpha_2^2\alpha_3^2)$$

Here K_o, K_1, and K_2 are the anisotropy constants characteristic of the material.

The Field Energy. In a uniform field consider a domain magnetized to saturation. Let the magnetization I_s be parallel to the applied field H. Then the energy per volume unit necessary to rotate the domain through θ to a new position with respect

to the field is,

$$E_H = \int_0^\theta I_s H \sin\theta \, d\theta = I_s H(1 - \cos\theta)$$

and the energy density is

$$E_H = -I_s H \cos\theta + \text{const}$$

The Magnetoelastic Energy. The derivation given here is from Becker and Döring (2), and is valid for materials having isotropic magnetostriction with no change of volume upon magnetization. Consider a small piece of this material cut in the form of a sphere of diameter ℓ while above its curie temperature. As it cools below its curie point, it becomes spontaneously magnetized into a single domain. Associated with this magnetization is a change in shape that may be represented to a first approximation by

$$\ell = A + B(\cos\phi)^2$$

where ℓ is the diameter measured in the direction making an angle ϕ with the direction of magnetization of the domain. Now consider a group of such domains oriented at random. Then the average length of a domain measured in any one direction in the group is

$$\bar{\ell} = A + B(\overline{\cos\phi})^2 = A + B/3$$

When the material is fully magnetized so that all domains are oriented in one direction, the length ℓ_o of each domain in the direction of magnetization of the group is

$$\ell_o = A + B$$

Now let $\lambda = \dfrac{\ell - \bar{\ell}}{\bar{\ell}}$ and $\lambda_s = \dfrac{\ell_o - \bar{\ell}}{\bar{\ell}}$

Then $$\frac{\lambda}{\lambda_s} = \left[(\cos \phi)^2 - 1/3\right]\frac{3}{2}$$

Hence $$\lambda = \frac{3}{2}\ \lambda_s \left[(\cos \phi)^2 - \frac{1}{3}\right]$$

In this relation λ represents the relative change in length (magnetostriction) of the material in a direction making an angle ϕ with the magnetization vector of the material. λ_s represents the relative change in the length when all domains are parallel (saturation magnetostriction).

The strain energy for a unit volume of the material can be evaluated by letting the change in length take place in the presence of an external constant tension σ, as the domains are rotated from their original position $\phi = \phi_o$ to $\phi = 0$.

$$E_\sigma = -\sigma\lambda = -\sigma 3/2\ \lambda_s \left[(\cos \phi)^2 - 1/3\right]$$
$$= -3/2\,\sigma\lambda_s \left[2/3 - (\sin \phi)^2\right]$$
$$E_\sigma = 3/2\,\sigma\lambda_s\ (\sin \phi)^2 - \sigma\lambda_s$$

If the magnetostriction is positive as in iron and a tension is applied ($\sigma_2 > 0$), the energy is minimum for $\phi = 0$. Therefore tension causes the magnetization to be parallel to the axis of tension. For negative magnetostriction as in nickel, the energy is minimum when $\phi = \pi/2$. Therefore tension causes the magnetization to be perpendicular to the direction of stress.

THE THEORETICAL LONGITUDINAL MAGNETIZATION CURVE

The theoretical determination of the magnetization curve of a stressed ferromagnetic material over the range $-\infty < H < \infty$ is

a complex problem and can be solved only after some highly restrictive simplifications. Consider, for instance, the case of a wire under tension and torsion, with the applied field parallel to the axis of the wire. Suppose the wire to be magnetized to saturation in the upward direction. As the magnetic intensity decreases to zero, the magnetization will decrease to I_r. Theoretical considerations not given explicitly in this thesis indicate that when the magnetic intensity is increased in the opposite direction, the first portion of the wire to change its magnetization toward the new direction of H is a small diameter ($\rho_c << 1$) cylinder concentric with the axis. As H increases, the diameter of this cylinder of reversed magnetization increases until for some distinct value of H, dependent on the parameters tension and torque, the remaining unreversed cylinder no longer changes its magnetization by reversible rotation and Block wall displacement, but instead undergoes a discontinuous rotation. The wire is then essentially one single macroscopic domain, and as the applied field increases further the change in magnetization in the wire again takes place by reversible rotation.

It is difficult to represent mathematically the energies and domain wall movements and specifically the longitudinal and circular magnetization as a function of the applied field, torque, and tension for a process such as described above. To simplify the situation and initiate investigations in this problem, the writer chose to consider only the reversible region $H \geq 0$. As a result, the theory outlined below is strictly valid only for reversible rotations.

It is always possible to replace all stresses acting on an isotropic body by three mutually perpendicular stresses which are referred to as the "principal" stresses. In the appendix the determination of the directions and magnitudes of the principal stresses in a torqued cylinder are presented in detail. The analysis shows that there are only two directions of stress, one compressive and the other tensile. Both make an angle of 45 degrees with the axis of the cylinder and both are perpendicular to the radius vector which is perpendicular upon the axis of the cylinder. For a material with a positive linear saturation magnetostriction constant, the action of the compressive stress with regard to the magnetoelastic energy term is equivalent to a perpendicular tensile stress of equal magnitude. Hence the expression for E_σ becomes

$$E_\sigma = 3\lambda_s \sigma (\sin \phi)^2 \qquad (1)$$

To make tenable the derivation of the magnetization curve and present a reasonably simple model of the magnetization process, it is assumed that internal stresses are negligible and that either the texture (degree of preferred crystal orientation) is zero, or E_k is zero. The total energy density expression is then

$$E_T = E_\sigma + E_H \qquad (2)$$

Minimization of this expression leads to the component expressions for the equations of magnetization.

$$I_H = I_s \cos \theta \qquad (3a)$$

$$H = 3G \frac{d\phi}{d\ell} \rho\left(\frac{\lambda_s}{I_s}\right) \frac{\cos 2\theta}{\sin \theta} \qquad (3b)$$

θ is the angle between the direction of I_s and a line parallel to the axis of the cylinder, G is the shear modulus, $\frac{d\phi}{d\ell}$ the angular displacement per unit length, and ρ the radius vector from the axis of the cylinder. It is seen that the parametric equation for H is a function of ρ. The expression for the longitudinal magnetization in the rod is

$$I_L = \frac{1}{r^2\pi} \int_0^r I_s \cos\theta \, 2\pi\rho \, d\rho \qquad (4)$$

If ρ as a function of θ is substituted in (4) and the resulting integral evaluated from 1 to $u_o = \cos\theta_o$ (where θ_o is the value of θ at $\rho = r$), the parametric equations of magnetization for the torqued cylinder become

$$I_L = I_s \left[\frac{2u_o^2 - 1}{(1 - u_o^2)^{\frac{3}{2}}}\right]^2 \left[u_o\left(\frac{1 - u_o^2}{(2u_o^2 - 1)^2}\right) + \frac{3}{8\sqrt{2}} \ell n \left(\frac{\sqrt{2}u_o - 1}{\sqrt{2}u_o + 1}\right)\left(\frac{\sqrt{2} + 1}{\sqrt{2} - 1}\right) + \frac{1}{4}\left(\frac{u_o}{2u_o^2 - 1} - 1\right)\right] \qquad (5a)$$

$$H = 3Gr \frac{\lambda_s}{I_s} \frac{d\phi}{d\ell} \frac{2u_o^2 - 1}{(1 - u_o^2)t} \qquad (5b)$$

Plate VI is a plot of (5a) and (5b) for $0 \leq \theta \leq 45°$, with $G = 5.87 \times 10^{11}$ dyne/cm^2, $\lambda_s = 23.9 \times 10^{-6}$, $I_s = 16{,}000/4\pi$ pole/cm^2, $r = 1.27 \times 10^{-2}$ cm, and $\frac{d\phi}{d\ell}$ in multiples of $2\pi/110$ cm, i.e., one turn corresponds to a displacement of 2π radians per 110 cm.

If the parameter u_o is eliminated between (5a) and (5b), it is seen that I_1 is a function only of $\frac{H}{d\phi/d\ell}$. Besides a comparison between the theoretical and experimental values of ΔI_1, it

was an objective of this thesis to check on the functional dependence of I_1 upon $\frac{H}{d\phi/d\ell}$.

THE EXPERIMENTAL METHOD

General Principle

In principle the measurement of the longitudinal component of magnetization is not difficult. The standard method employs a field producing solenoid and a search coil coaxial with the field coil. The specimen is placed in the field coil and its magnetization changed by changing the magnitude and/or direction of the current in the field coils. Accompanying the change of magnetization will be an induced emf in the search coil, given by

$$\mathcal{E} = -N \frac{d\phi}{dt}$$

If $\mathcal{E}$ is due only to the change in magnetization, then

$$\Delta I_L = \frac{10^8}{AN\ 4\pi} \int_{t_1}^{t_2} \mathcal{E}\, dt = \frac{B - H}{4\pi}$$

In this formula A is the cross-sectional area of the specimen in cm^2, N is the number of turns in the search coil. $\mathcal{E}$ is expressed in volts, t in seconds, and I_1 in unit poles/cm^2.

In this work the demagnetization field of the specimen in the region of the search coil is negligible.

To a sufficient degree of approximation (three places) the magnetic field in the region of the search coils is given by

$$H = \frac{Ni\ 4\pi}{10}$$

where N is in turns/cm, and i is in amperes.

Since the search coil is located at approximately the center of the field coil, the flux linkage coefficient is assumed to be 1.

The Basic Apparatus

A sketch of the basic apparatus is given in Plate II. Plate III is a schematic of the experimental set-up. The field coils K and L shown in Plate II are physically identical. Each is 89.52 ± 0.10 cm long and of mean diameter 1.05 cm, and has 1040 turns. The search coils J and I are very nearly identical, each containing 5000 turns. The average outside diameter is 3.73 cm, while the inside diameter of each is 2.52 cm and their length is 3.89 ± 0.04 cm.

The RC Integrator

The circuit used for the integration of the search coil voltage is shown in (2) of Plate I. The voltage across C due to the input voltage $V_i(t)$ is given generally by

$$V_o(t) = \frac{e^{-t/RC}}{RC} \int_o^t V_i(t) e^{t/RC} dt + V_{oo} e^{-t/RC}$$

When $V_i(t) = V_i(t + T)$, then $V_o(t) = V_o(t + T)$ for the steady-state condition. To a first approximation the relationship

between the time integral of the input voltage and the output voltage $V_o(t)$ is given by

$$\int_o^t V_i dt = RC\ V_s(t)$$

where the point $t = 0$ is chosen so that $V_o(0) = 0$.

Calibration of the Integrator

Figure 2 of Plate IV shows the functional change in $V_i(t)$ (the voltage across the search coils) which is characteristic of the polarized wires used in this work. The range of H in these photographs is approximately 20 to 120 oersteds (see Plate explanation). Over the range $0 \leq H \leq 120$ oersteds torsion, longitudinal stress, and degree of polarization do not significantly affect the manner in which the function V_i changes. The wave forms shown here are for a polarized wire under a stress of 1 kg/mm^2, and no torsional stress.

To calibrate the integrator it will be assumed that the relation between V_i and V_s can be represented by

$$\int_o^t V_i(t)\ dt = k(V_i)\ RC\ V_s(t)$$

In this expression k varies with different V_i. $RC\ k(V_i)$ has been determined experimentally for nine different wave forms of V_i distributed uniformly over the range of H used in this work. The "calibration curve" thus obtained is shown in Plate V. Since the curve is nearly linear, it has been assumed that $k(V_i)$ is a constant, namely, the graphical average of $k(V_i)$ over the different V_i. The error thus introduced is small. Experimentally,

RC $k(V_i)_{ave}$ = 2.44 x 10^{-4} volt-sec/millivolt. In the integrator R = .43300 megohm, and C = .538 μfd; hence RC = 2.33 x 10^{-4} volt-sec/millivolt.

The phase shift between the wave form of V_s and that of the applied field, caused by the integrator and associated circuitry, has been found to be negligible. Figure 4 of Plate IV is a photograph displaying V_s along the vertical axis, and V_h (the voltage across a resistance in the field coil circuit) along the horizontal axis. This is a check on the phase shift between V_s and V_h. The vertical and horizontal amplifiers were a matched set and had identical coupling constants.

Determination of the Wire Constants

The saturation linear magnetostriction constant for 51 per cent Ni-49 per cent Fe wires under a longitudinal stress of 2.74 kg/mm^2 has been measured and found to be 23.9 x 10^{-6}. A microscope was mounted at right angles to the axis of the wire, near the bottom of the field coils of the apparatus, and the transient change in length of the wire upon magnetization was observed by using a microcomparator type eye piece in conjunction with the microscope. The measured value of λ_s is in good agreement with the values obtained by other workers (see Bozorth, page 671).

The diameter of the wire was measured using this same microscope arrangement and found to be .253 mm.

The isothermal shear modulus was measured using the torsional pendulum method and found to be 5.87 x 10^{11} $dynes/cm^2$.

Only one sample of wire was used; hence the measurement is not truly representative of the samples. Van der Maas has obtained the value 5.94×10^{11} in measurements involving several wires of different length.

A saturation induction (B - H) of 15,400 gauss has been measured for the wires used in this work. The accepted saturation induction for 51 per cent Ni - 49 per cent Fe alloys is 16,000 gauss. The saturation magnetization in cgs units is, then, $I_s = 15{,}400/4\pi$ poles/cm^2. A general method of obtaining I_s involves plotting (B - H) as a function of 1/H, and extrapolating to $H = \infty$. The degree of error introduced in the extrapolation is dependent on the range of H values. In the measurements reported here the largest value of H used was approximately 45 oersteds. Hence the extrapolation error probably accounts for some of the discrepancy between the measured and accepted value (see Bozorth, page 870).

Polarization of the Specimen

The Problem. In the ideal case (no texture and no internal stress), the polarization of a polycrystalline ferromagnetic may be accomplished by subjecting it to an intense magnetic field. When texture and internal stress are present, as is the case in all fabricated metals, the meaning of the term polarization is somewhat ambiguous in that the remanent magnetization may vary considerably, depending on the internal structure of the material, i.e., the internal stresses and texture. From the theory

outlined above it is clear that in this work polarization will mean that no regions of reversed magnetization are present in the specimen, that is to say it is essentially on macrodomain. It is difficult to determine when the specimen meets this requirement, since the internal stresses and texture are usually not known. Initial measurements on the specimens used here show that subjecting the wire to a magnetic field of 150 oersteds does not polarize it.

Magnetic Annealing. In this work a method of magnetic annealing has been used to obtain high degrees of polarization. Ordinary annealing relieves internal stresses. Annealing under stress reorients the internal stresses. In the magnetic annealing process used here, the wire was placed in the field coil of the apparatus and heated until its temperature exceeded its curie point temperature. An electric current applied across the specimen provided the means to heat the wire. After an equilibrium temperature was reached (approximately 10 seconds after the current has been applied to the wire), the field coil was energized to produce a longitudinal magnetic field of 165 oersteds. Then the current through the sample was cut off, and the sample was allowed to cool rapidly (4-5 seconds) through its curie point to room temperature while in a constant longitudinal magnetic field and under a constant tensile stress. Rapid cooling is objectionable because of the possibility of introducing large internal stresses. However, it is necessary because maintaining the annealing current in the wire would retain an unwanted circular component of magnetic field. When the wire had reached

room temperature, the magnetic field was decreased continuously from 165 oersteds to 7 or 8 oersteds.

Comparison of data from magnetically annealed wires, and wires polarized below their curie point after being annealed under longitudinal stress, shows that the magnetic annealing does not measurably change the texture of the sample.

RESULTS

Plates VII through XII display the experimentally obtained relationships between ΔI_1 and H for different values of the parameters, polarizing stress, longitudinal stress, and torque. Comparison of these curves with the theoretical curves (Plate VI) shows qualitative agreement with the simple theoretical model. A precise quantitative comparison is difficult for the following reasons: (a) The exact nature of the internal stresses before and after polarization is not known, and (b) the texture of the samples before and after polarization is not accurately known. Both these factors influence the magnetization, and neither is taken into consideration in the simple model. Measurements of the longitudinal magnetization of samples under large external longitudinal stress (20.3 kg/mm^2) show the existence of a curve for $\frac{d\phi}{d\ell} = 0$. At this value of longitudinal stress the internal stresses are surely negligible and we must attribute the existence of the curves for $\frac{d\phi}{d\ell} = 0$ to the fact that the texture and internal stress are not negligible.

Consider now the predicted relationship between ΔI_1 and $\frac{H}{d\phi/d\ell}$ for the case of zero longitudinal stress. It has been shown that theoretically $\Delta I_L = g(\frac{H}{d\phi/d\ell})$. Plate XIII displays a plot of ΔI_1 versus $(\frac{H}{d\phi/d\ell})$ for the data shown in Plate XI. This plot is representative for those obtained from other data, e.g., Plate XII. It is seen from this set of curves that I_1 is very nearly a function of $\frac{H}{d\phi/d\ell}$ only. Plots of the experimental versus the theoretical magnetization (Plates XIV through XVII) are to the first order linear, and reveal that the polarizing stress influences both the linearity and the slope. The slope measures the degree of departure between the theoretical and experimental magnitudes of ΔI_1. The linearity of these plots may be considered to measure the experimental validity of the relation $\Delta I_L = g(\frac{H}{d\phi/d\ell})$.

CONCLUSIONS

The simple model of the magnetization mechanism suggested here appears to hold promise of describing the reversible quasi-static magnetization processes in stressed ferromagnetics. Results presented show that the model is not unreasonable even when internal stress and texture are not negligible. Further investigations of both the longitudinal and circular components of the magnetization of different ferromagnetic materials would test more severely the adequacy of the proposed theoretical model of the magnetization mechanism.

ACKNOWLEDGMENTS

The writer would like to express his sincere appreciation to Dr. G. J. van der Maas for his inspiration and guidance in this work. Special thanks are also extended to Mr. A. E. Asch, who worked with the writer, and is conducting similar investigations on the circular magnetization in torqued nickel-iron wires. Mr. L. W. Phillips provided valuable assistance in the construction of the apparatus.

LITERATURE CITED

1. Akulov, N. S. Z.
   Atomic theory of ferromagnetism. Z. Physik. 54:582-7. 1929.

2. Becker, R. and W. Doring.
   Ferromagnetismus. Berlin: J. Springer, 1939.

3. Bitter, F.
   On inhomogeneities in the magnetization of ferromagnetic materials. Phys. Rev. 38:1903-05. 1931.

4. Bozorth, R. M.
   Ferromagnetism. New York: D. Van Nostrand, 1950.

5. Dijkstra, L. J. and J. L.
   Propagation of large Barkhausen discontinuities in Fe-Ni alloys. Phillips Res. Rep. 4:334. 1949.

6. Joule, J. P.
   On the effects of magnetism on the dimensions of iron and steel bars. Philosophical Magazine. 30:76-87, 225-241. 1847.

7. Laudau, L. and E. Lifshitz.
   Theory of dispersion of magnetic permeability in ferromagnetic bodies. Physik Z. Sowjetunion. 8. 1935.

8. Sixtus, K. L. and L. Tonks.
   Propagation of large Barkhausen discontinuities. Phys. Rev. 37:930-58. 1931.

9. Stewart, K. H.
   Experiment on a specimen with large domain. J. Phys., Radium. 12:325. 1951.

10. van der Maas, G. J.
    Quarterly progress reports, National Research Council, Canada. 1949, et seq.

11. van der Maas, G. J.
    Private communication, 1959.

12. Williams, H. J., R. M. Bozorth, and W. Shockely.
    Magnetic domains in single crystals of silicon iron. Phys. Rev. 75:155-78. 1949.

APPENDICES

APPENDIX I

Determination of the principal directions of stress in a torqued wire

Consider the symmetric stress tensor

$$(S) = \begin{bmatrix} X_x & Y_x & Z_x \\ X_y & Y_y & Z_y \\ X_z & Y_z & Z_z \end{bmatrix} \qquad Y_x = X_y \quad Z_x = X_z \quad Y_z = Z_y$$

In this expression an arbitrary element, say Z_y, represents the force in the Z direction on a surface whose normal is in the y direction. It is desired to know the three directions of pure normal stress and the corresponding stress values X_n, Y_n, and Z_n which describe completely the stressed condition of the body. This is equivalent to the determination of the directions α, β, and γ, for which

$$(S) \begin{bmatrix} \cos\alpha \\ \cos\beta \\ \cos\gamma \end{bmatrix} = \lambda \begin{bmatrix} \cos\alpha \\ \cos\beta \\ \cos\gamma \end{bmatrix} \quad \text{where } \lambda \begin{bmatrix} \cos\alpha \\ \cos\beta \\ \cos\gamma \end{bmatrix} = \begin{bmatrix} X_n \\ Y_n \\ Z_n \end{bmatrix}$$

Expanding and rewriting,

$$\left.\begin{aligned} (X_x - \lambda)\cos\alpha + Y_x\cos\beta + Z_x\cos\gamma &= 0 \\ X_y\cos\alpha + (Y_y - \lambda)\cos\beta + Z_y\cos\gamma &= 0 \\ X_z\cos\alpha + Y_z\cos\beta + (Z_z - \lambda)\cos\gamma &= 0 \end{aligned}\right\} \qquad (1)$$

Solutions of (1) will be non-trivial only if

$$\begin{vmatrix} (X_x - \lambda) & Y_x & Z_x \\ X_y & (Y_y - \lambda) & Z_y \\ X_z & Y_z & (Z_z - \lambda) \end{vmatrix} = 0 \qquad (2)$$

For a cylindrical wire under torsion with its axis along Z, the tensor elements are

$$Y_z = G \frac{d\phi}{d\ell} x = Z_y, \quad X_z = -G \frac{d\phi}{d\ell} y = Z_x$$

$$X_x = Y_y = Z_z = 0, \quad X_y = Y_x = 0$$

Here G is the isothermal shear modulus, and $\frac{d\phi}{d\ell}$ represents the angular displacement per unit length. Substituting these values in (2) yields,

$$\begin{vmatrix} -\lambda & 0 & -G \frac{d\phi}{d\ell} y \\ 0 & -\lambda & G \frac{d\phi}{d\ell} x \\ -G \frac{d\phi}{d\ell} y & G \frac{d\phi}{d\ell} x & -\lambda \end{vmatrix} = 0 \qquad (2a)$$

Solving for λ it is found that

$$\lambda_1 = G \frac{d0}{d\ell} \rho, \quad \lambda_2 = -G \frac{d\phi}{d\ell} \rho, \quad \lambda_3 = 0$$

where $\rho = (x^2 + y^2)^{\frac{1}{2}}$. Since $\lambda_3 = 0$, there are only two non-degenerate principal directions of stress. Substituting λ_1 in (1) gives

$$\frac{\cos \alpha_1}{\cos \gamma_2} = -\frac{y}{\rho} \quad \text{and} \quad \frac{\cos \beta_1}{\cos \gamma_1} = \frac{x}{\rho} \qquad (3)$$

Substituting λ_2 in (1) gives

$$\frac{\cos \alpha_2}{\cos \gamma_2} = -\frac{y}{\rho} \quad \text{and} \quad \frac{\cos \beta_2}{\cos \gamma_2} = -\frac{x}{\rho} \qquad (4)$$

Using $(\cos \alpha)^2 + (\cos \beta)^2 + (\cos \gamma)^2 = 1$

one obtains from (2) and (3)

$$\cos \gamma_1 = \pm \frac{1}{\sqrt{2}} \qquad \cos \gamma_2 = \pm \frac{1}{\sqrt{2}}$$

Letting $\cos \gamma_1 = + \frac{1}{\sqrt{2}}$ and $\cos \gamma_2 = - \frac{1}{\sqrt{2}}$ yields

$$\cos \alpha_1 = \frac{-y}{\sqrt{2}\rho} \quad \cos \beta_1 = \frac{x}{\sqrt{2}\rho} \quad \cos \gamma_1 = \frac{1}{\sqrt{2}} \quad \gamma_1 = \frac{\pi}{4}$$

and

$$\cos \alpha_2 = \frac{-y}{\sqrt{2}\rho} \quad \cos \beta_2 = \frac{x}{\sqrt{2}\rho} \quad \cos \gamma_2 = \frac{-1}{\sqrt{2}} \quad \gamma_2 = - \frac{\pi}{4}$$

The principal stresses are therefore

$$X_1 = - \frac{d\phi}{d\ell} \frac{y}{\sqrt{2}} G \qquad X_2 = \frac{d\phi}{d\ell} \frac{y}{\sqrt{2}} G$$

$$Y_1 = \frac{d\phi}{d\ell} \frac{x}{\sqrt{2}} G \qquad Y_2 = - \frac{d\phi}{d\ell} \frac{x}{\sqrt{2}} G$$

$$Z_1 = \frac{d\phi}{d\ell} \frac{\rho}{\sqrt{2}} G \qquad Z_2 = - \frac{d\phi}{d\ell} \frac{\rho}{\sqrt{2}} G$$

and $\sigma_i = (X_i^2 + Y_i^2 + Z_i^2)^{\frac{1}{2}} = G \frac{d\phi}{d\ell} \rho$

Determination of the Longitudinal Magnetization Curves of a Torqued Wire

It is assumed that the total energy expression is given by

$$E_T = E_\sigma + E_H$$

Let the applied field be parallel to the axis of the wire as in (1) of Plate I. Then E_t becomes

$$E_T = 3\sigma \lambda_s \left[\sin(45^\circ - \theta)\right]^2 - I_s H \cos \theta \qquad (1)$$

and

$$\frac{dE_T}{d\theta} = -6\sigma\lambda_3 \cos(45^\circ - \theta) \sin(45^\circ - \theta) + I_s H \sin\theta = 0 \qquad (2)$$

Solving (2) for H, one obtains the component equations of magnetization, namely,

$$I_H = I_s \cos\theta \qquad (2a)$$

$$H = \frac{3\sigma\lambda_s \cos 2\theta}{I_s \sin\theta} \qquad (2b)$$

These equations are valid only for those values of θ for $\frac{d^2E_T}{d\theta^2} > 0$.

Let it be required to minimize the general expression

$$f(\theta) - H I_s \cos\theta$$

For a minimum

$$f'(\theta) + I_s H \sin\theta = 0 \qquad (3a)$$

$$f''(\theta) + I_s H \cos\theta > 0 \qquad (3b)$$

From (2a) and (3a) one can write

$$dI = -I_s \sin\theta \, d\theta$$

$$dH = -\frac{(H I_s \cos\theta + f''\theta)}{I_s^2 \sin\theta} d\theta$$

Hence for (2) to be a minimum it must be true that

$$\frac{dI}{dH} = \frac{(I_s \sin\theta)^2}{(I_s H \cos\theta + f''(\theta))} > 0$$

The total longitudinal flux can be obtained by integrating (2a) over the cross-sectional area of the wire. Thus

$$\phi_t = \int_0^r I_s \cos\theta \, 2\pi\rho \, d\rho$$

Letting $u = \cos\theta$, and substituting

$$\rho = \rho(\theta) = \frac{I_s H\,(1 - u^2)^{\frac{1}{2}}}{3\lambda_G \dfrac{d\phi}{d\ell}\,(2u^2 - 1)}$$

in (4) yields

$$\phi_t = \pi I_s \left(\frac{I_s H}{3\lambda_s\, G\, \dfrac{d\phi}{d\ell}}\right)^2 \int_{u_1}^{u_2} u\, d\left[\frac{(1 - u^2)}{(2u^2 - 1)^2}\right] \qquad (4)$$

where $u_1 = +1$, and $u_2 = \cos\theta_o$.

Putting $$A = \pi I_s \left(\frac{I_s H}{3\lambda_s\, G\, \dfrac{d\phi}{d\ell}}\right)^2$$

(4) becomes

$$\phi_t' = \frac{\phi_t}{A} = \int_1^{u_o} u\, d\left[\frac{1 - u^2}{(2u^2 - 1)^2}\right]$$

Integrating by parts gives

$$\phi_t' = u\,\frac{1 - u^2}{(2u^2 - 1)^2}\Bigg|_1^{u_o} - \int_1^{u_o} \frac{(1 - u^2)\,du}{(2u^2 - 1)^2} \qquad (5)$$

But

$$\int \frac{(1 - u^2)\,du}{(2u^2 - 1)^2} = \tfrac{1}{2}\int \frac{du}{(2u^2 - 1)^2} - \tfrac{1}{2}\int \frac{du}{(2u^2 - 1)}$$

and $$\int_1^{u_o} \frac{du}{2u^2 - 1} = \frac{1}{2\sqrt{2}}\,\ell n\left(\frac{\sqrt{2}\,u - 1}{\sqrt{2}\,u + 1}\right)\Bigg|_1^{u_o}$$

Also $$\int_1^{u_o} \frac{du}{2u^2 - 1} = \frac{u}{2u^2 - 1}\Bigg|_1^{u_o} + \int_1^{u_o} \frac{4u^2\,du}{(2u^2 - 1)^2}$$

and $$\int_1^{u_o} \frac{u^2\,du}{(2u^2 - 1)^2} = \frac{1}{8\sqrt{2}}\,\ell n\,\frac{\sqrt{2}\,u - 1}{\sqrt{2}\,u + 1}\Bigg|_1^{u_o} + \frac{1}{4}\left(\frac{u}{2u^2 - 1}\right)\Bigg|_{u_o}^{1}$$

Therefore the complete integral is

$$\int_1^{u_o} \frac{1 - u^2}{(2u - 1)^2}\, du = -\frac{3}{8\sqrt{2}} \ell n \left(\frac{\sqrt{2}u_o - 1}{\sqrt{2}u_o + 1}\right)\left(\frac{\sqrt{2} + 1}{\sqrt{2} - 1}\right) - \frac{1}{4}\left(\frac{u_o}{2u_o^2 - 1} - 1\right)$$

and (5) becomes

$$\phi_t' = u_o \frac{1 - u_o^2}{(2u_o^2 - 1)^2} + \frac{3}{8\sqrt{2}} \ell n \frac{\sqrt{2}\, u_o - 1}{\sqrt{2}\, u_o + 1}\left(\frac{\sqrt{2} + 1}{\sqrt{2} - 1}\right) + \frac{1}{4}\left(\frac{u_o}{2\, u_o^2 - 1} - 1\right)$$

Substituting the expression for H in the expression for A gives

$$A = \pi I_s r^2 \left(\frac{2\, u^2 - 1}{(1 - u^2)^{\frac{1}{2}}}\right)^2$$

Substituting the expression for A in the equation for ϕ_t' gives

$$I_L = \frac{\phi_t}{\pi r^2} = I_s \left(\frac{2u_o^2 - 1}{(1 - u_o^2)^{\frac{1}{2}}}\right)^2 \left[u_o \frac{1 - u_o^2}{(2u_o^2 - 1)^2} + \frac{3}{8\sqrt{2}} \ell n \left(\frac{\sqrt{2}\, u_o - 1}{\sqrt{2}\, u_o + 1}\right)\left(\frac{\sqrt{2} + 1}{\sqrt{2} - 1}\right) + \frac{1}{4}\left(\frac{u_o}{2\, u_o^2 - 1} - 1\right)\right]$$

The parametric equations of the magnetization curves are then

$$I_L = I_s \left(\frac{\cos 2\theta_o}{\sin \theta_o}\right)^2 \left[\cos \theta_o \frac{\sin^2 \theta_o}{\cos^2 2\theta_o} + \frac{3}{8\sqrt{2}} \ell n \left(\frac{\sqrt{2} \cos \theta_o - 1}{\sqrt{2} \cos \theta + 1}\right)\left(\frac{\sqrt{2} + 1}{\sqrt{2} - 1}\right) + \frac{1}{4}\left(\frac{\cos \theta_o}{\cos 2\theta_o} - 1\right)\right]$$

$$H = \frac{3\, Gr\lambda_s}{I_s} \frac{d\phi}{d\ell} \frac{\cos 2\theta_o}{\sin \theta_o}$$

APPENDIX II

EXPLANATION OF PLATE I

Fig. 1. Diagram representing the relationship H, I_s, and σ at some value of ρ.

Fig. 2. Schematic of the integrating circuit.

PLATE I

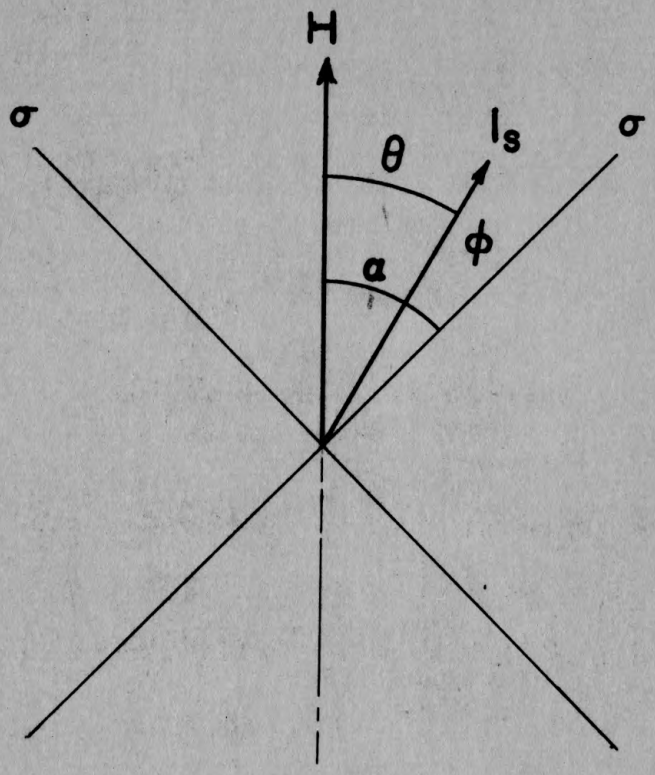

(1)

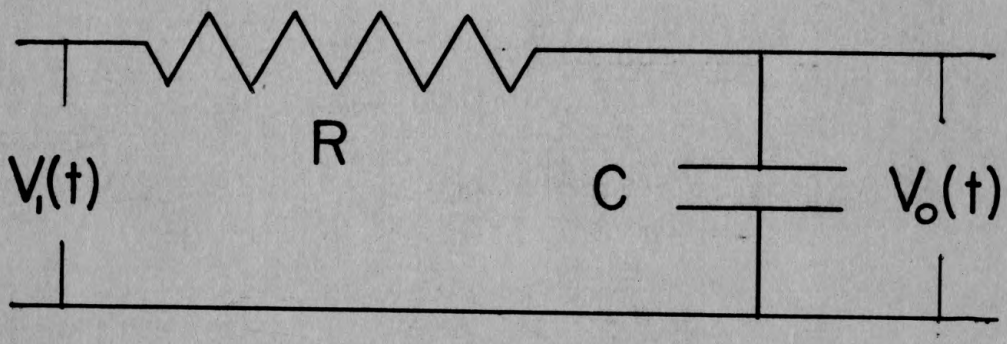

(2)

EXPLANATION OF PLATE II

Drawing of the Basic Apparatus

A. Torquing knob
B. 360° scale
C. Pointer
D. Leveling screws
E. Polyethelene insulator
F. Chuck
G. The sample
H. Location of the upper mercury contact
I. Search coil
J. Compensator search coil
K. Field coil
L. Compensator field coil
M. Search coil leads
N. Field coil leads
O. Mercury contact leads
P. Cap and body of contact
Q. Mercury pool
R. Platinum wire lead-outs
S. Location of lower mercury contact
T. Tab attached to sample
U. Lucite tab holder
V. Weight holder

PLATE II

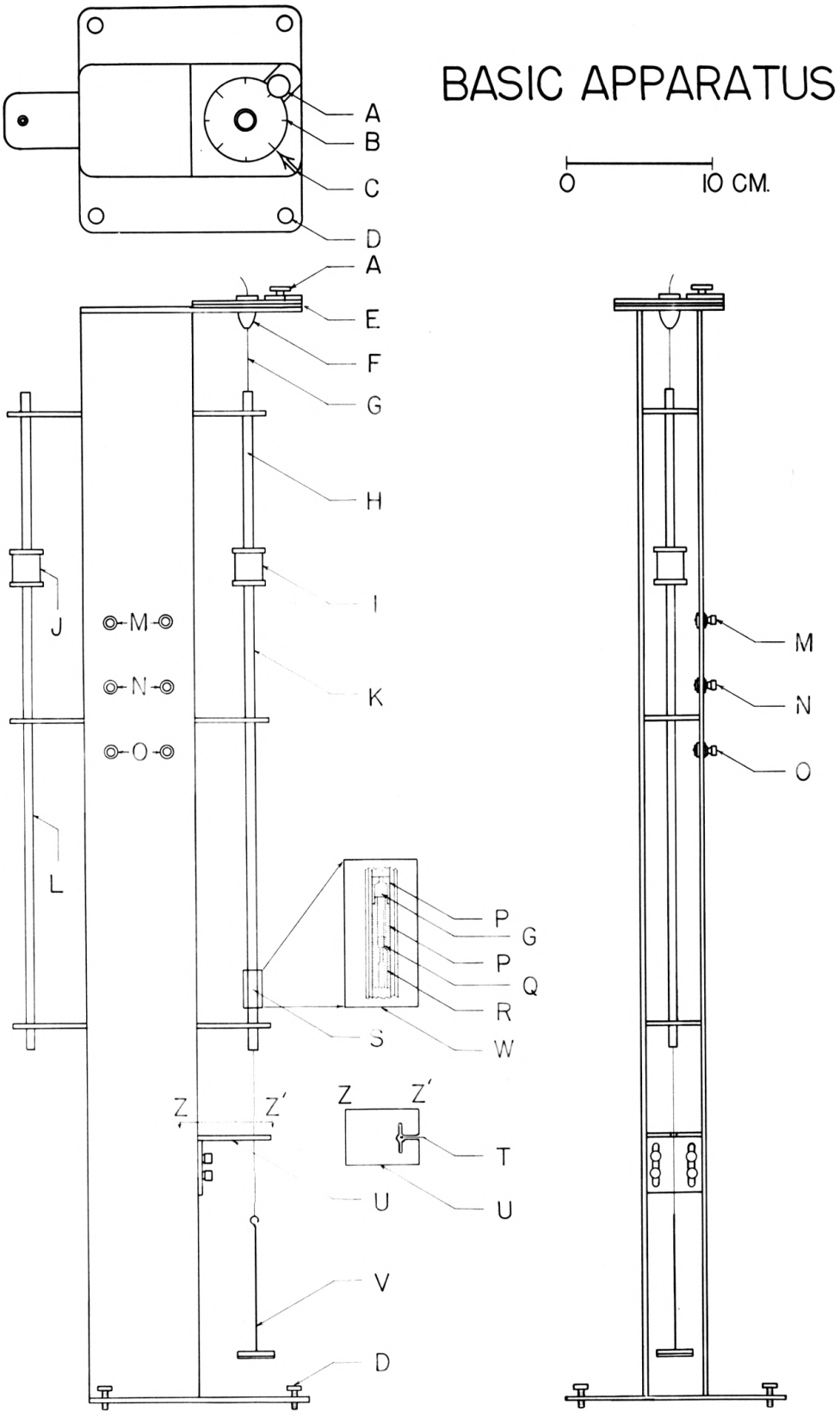
BASIC APPARATUS
0
10 CM.
A
B
C
D
A
E
F
G
H
I
J
M
N
O
K
L
P
G
P
Q
R
S
W
Z
Z'
T
U
U
V
D
M
N
O

EXPLANATION OF PLATE III

General Circuit Diagram of Experimental Set-up

A. Variac

B. Meters

C. Variable resistances

D. Half-wave rectifier

E. Mutual inductance

F. Compensator field coil

G. Field coil

H. Search coil

I. Compensator search coil

K. Integrating circuit

L. Oscilloscope

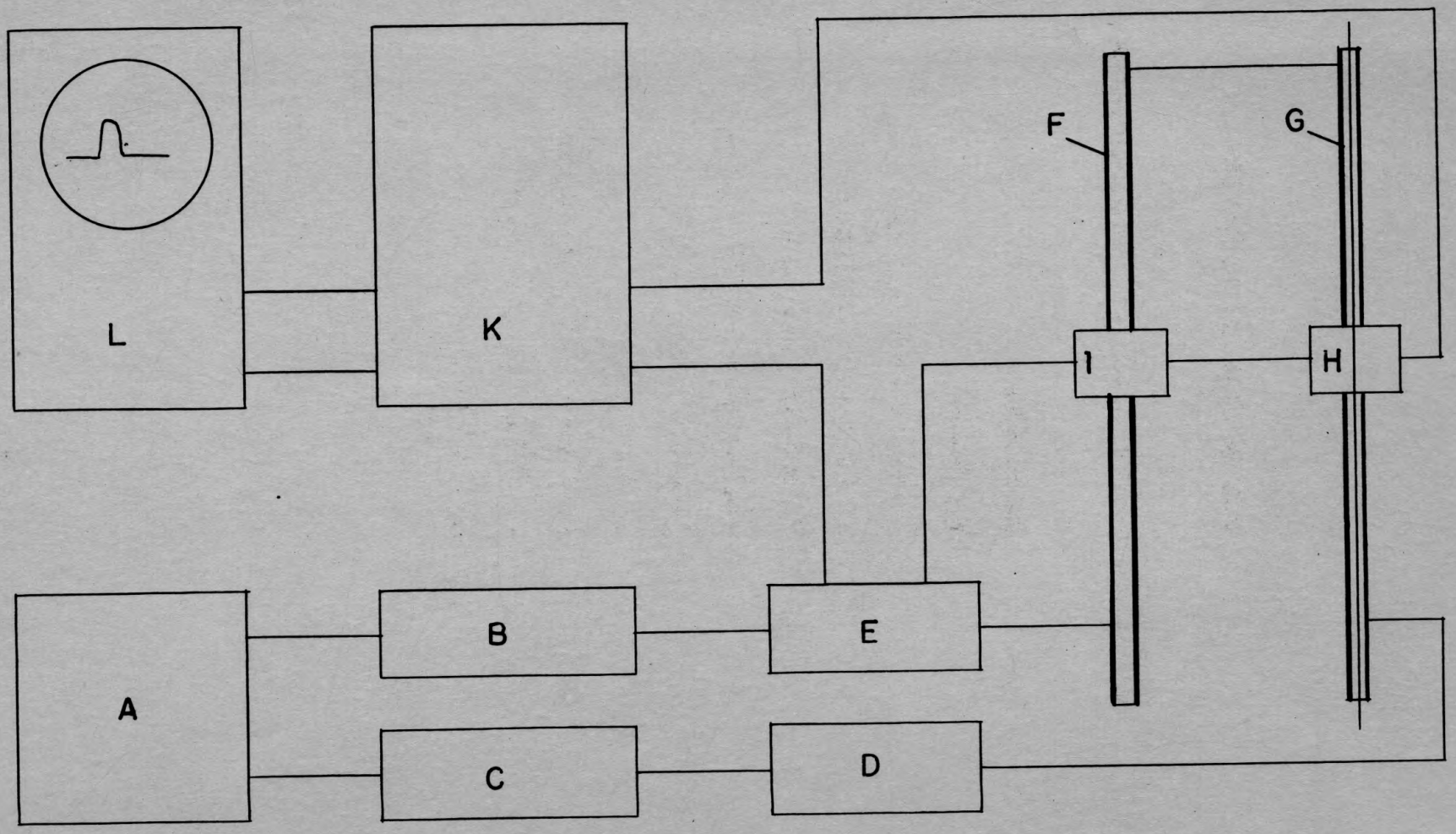

PLATE III

EXPLANATION OF PLATE IV

Fig. 1. The input wave form to the field coils.

Fig. 2. The input wave form to the integrator, i.e., the voltage across the search coils when specimen is in the field coil. Polarizing stress 5.93 kg/mm^2; longitudinal stress 1 kg/mm^2.

From the bottom reading up		H oersteds	V/cm
Time/cm = 2 ms/cm	a.	19.1	0.05
	b.	38.1	0.05
	c.	57.2	0.05
	d.	76.3	0.10
	e.	95.4	0.10

Fig. 3. Output wave form from integrator, same specimen as Fig. 2.

From bottom reading up		H oersteds	V/cm = .2 mv/cm
	a.	54.5	"
	b.	83.1	"
	c.	109	"
	d.	139	"
	e.	166	"

Fig. 4. V_h versus (horizontal) versus V_o (vertical) for different torques.

PLATE IV

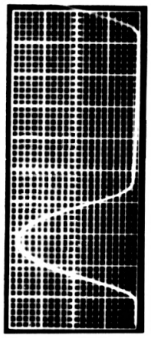

Fig. 1.

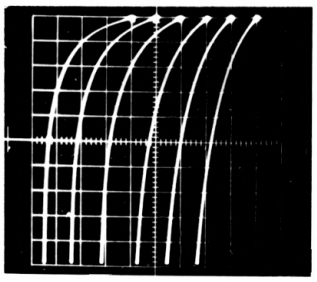

Fig. 4.

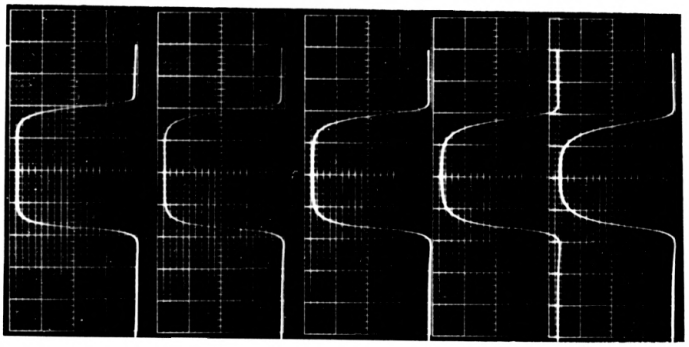

Fig. 3.

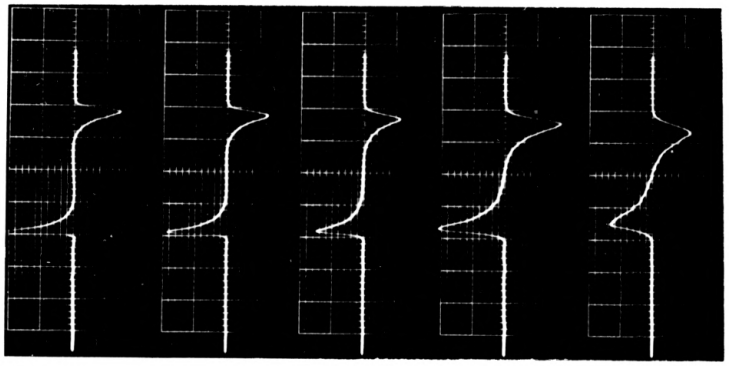

Fig. 2.

EXPLANATION OF PLATE V

The calibration curve for the integrating circuit

PLATE V

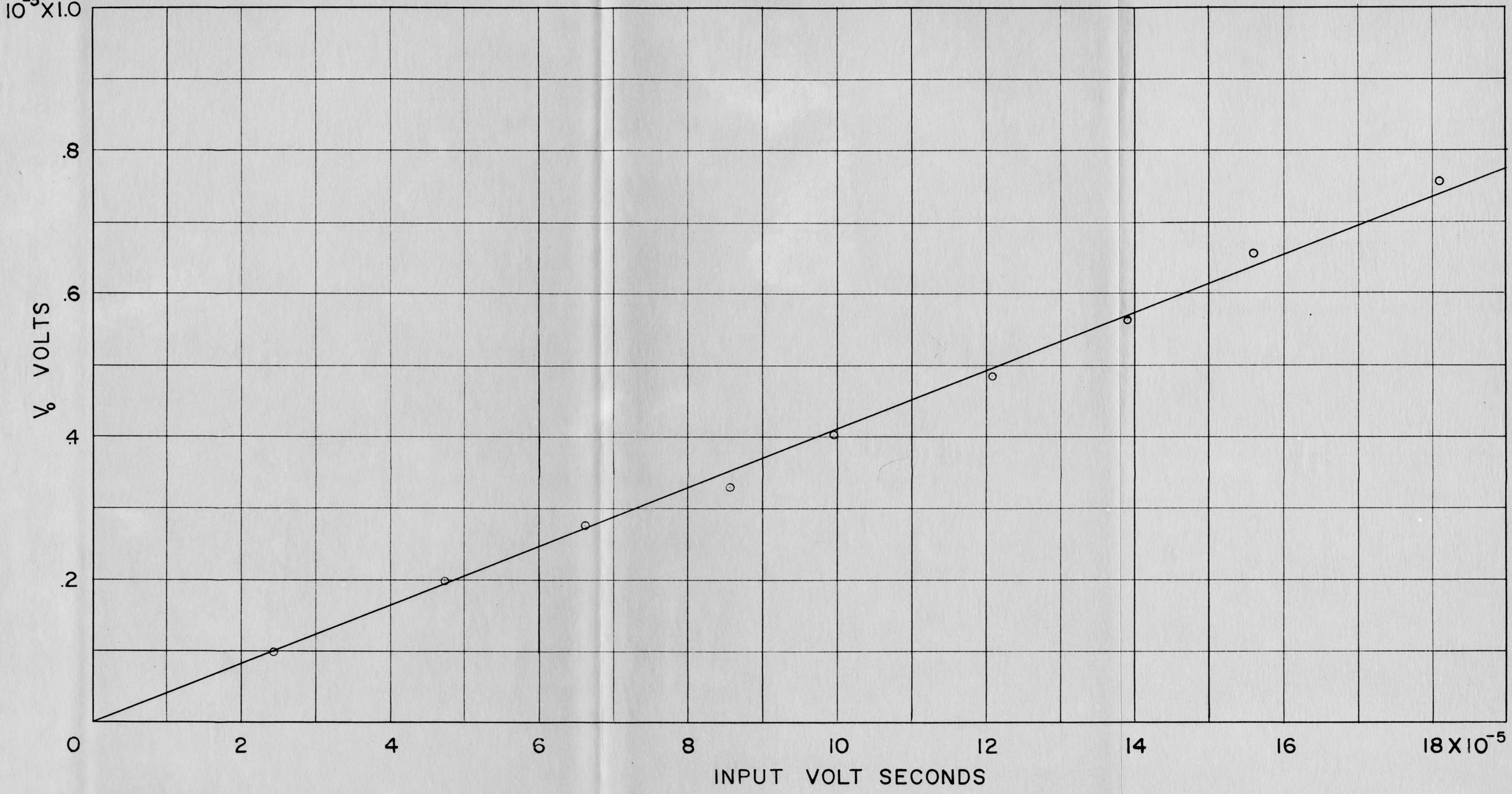
10^{-3}X1.0
.8
.6
.4
.2
V_o VOLTS
0
2
4
6
8
10
12
14
16
18X10^{-5}
INPUT VOLT SECONDS

EXPLANATION OF PLATE VI

The theoretical magnetization curves for a wire of the same dimensions as the experimental samples. The numbers denote angular displacement in turns per 110 cm. One turn = 3.27/cm.

PLATE VI

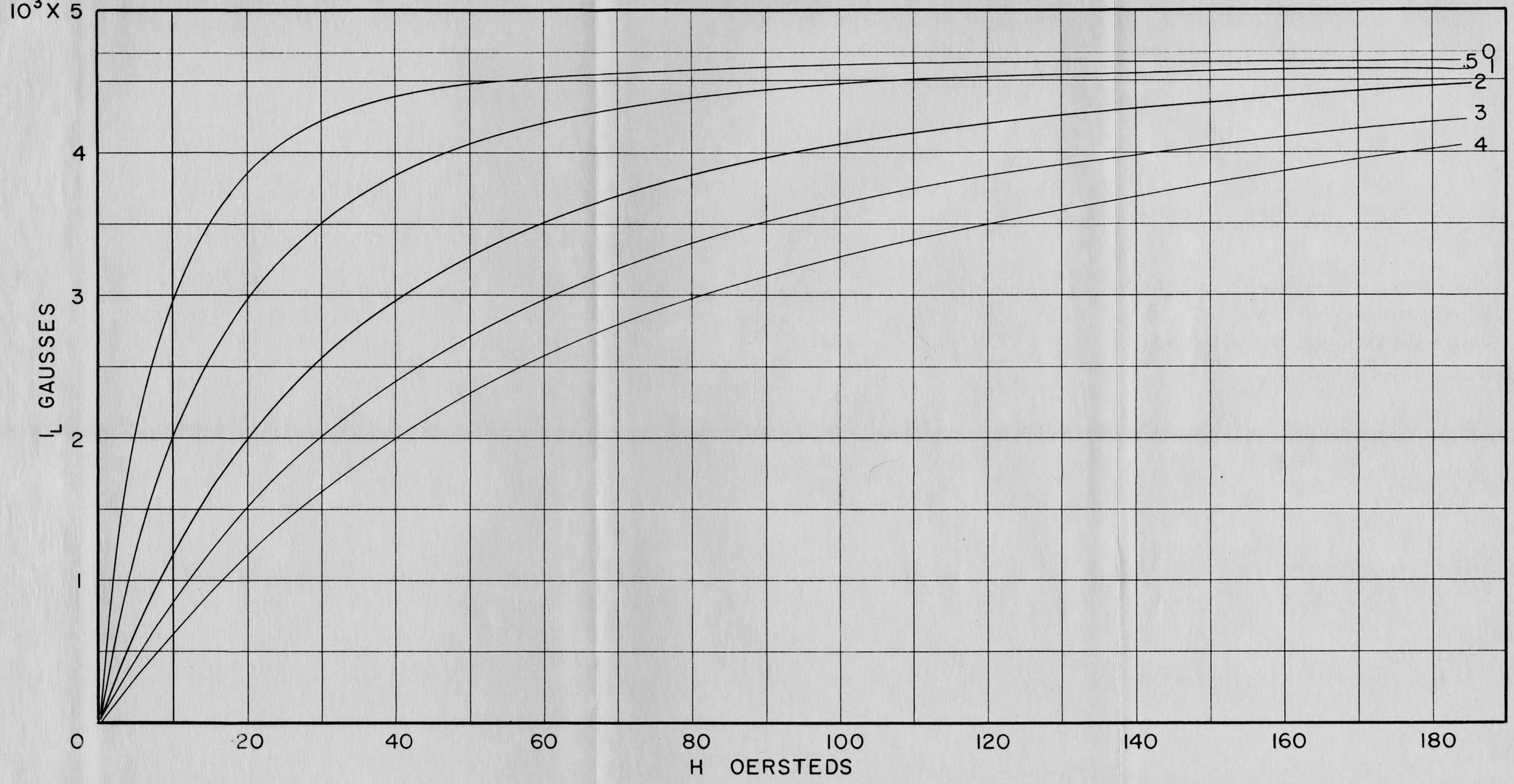
10^3 X 5
4
3
2
1
0
I_L GAUSSES
0
20
40
60
80
100
120
140
160
180
H OERSTEDS
0
.5
1
2
3
4

EXPLANATION OF PLATE VII

The experimental magnetization curves for different values of angular displacement (T). One turn (T) is equal to 3.27°/cm.

Wire No. 8

Polarizing stress	0.988 kg/mm^2
Longitudinal stress	0.988 kg/mm^2
Polarizing field	167 oersteds

PLATE VII

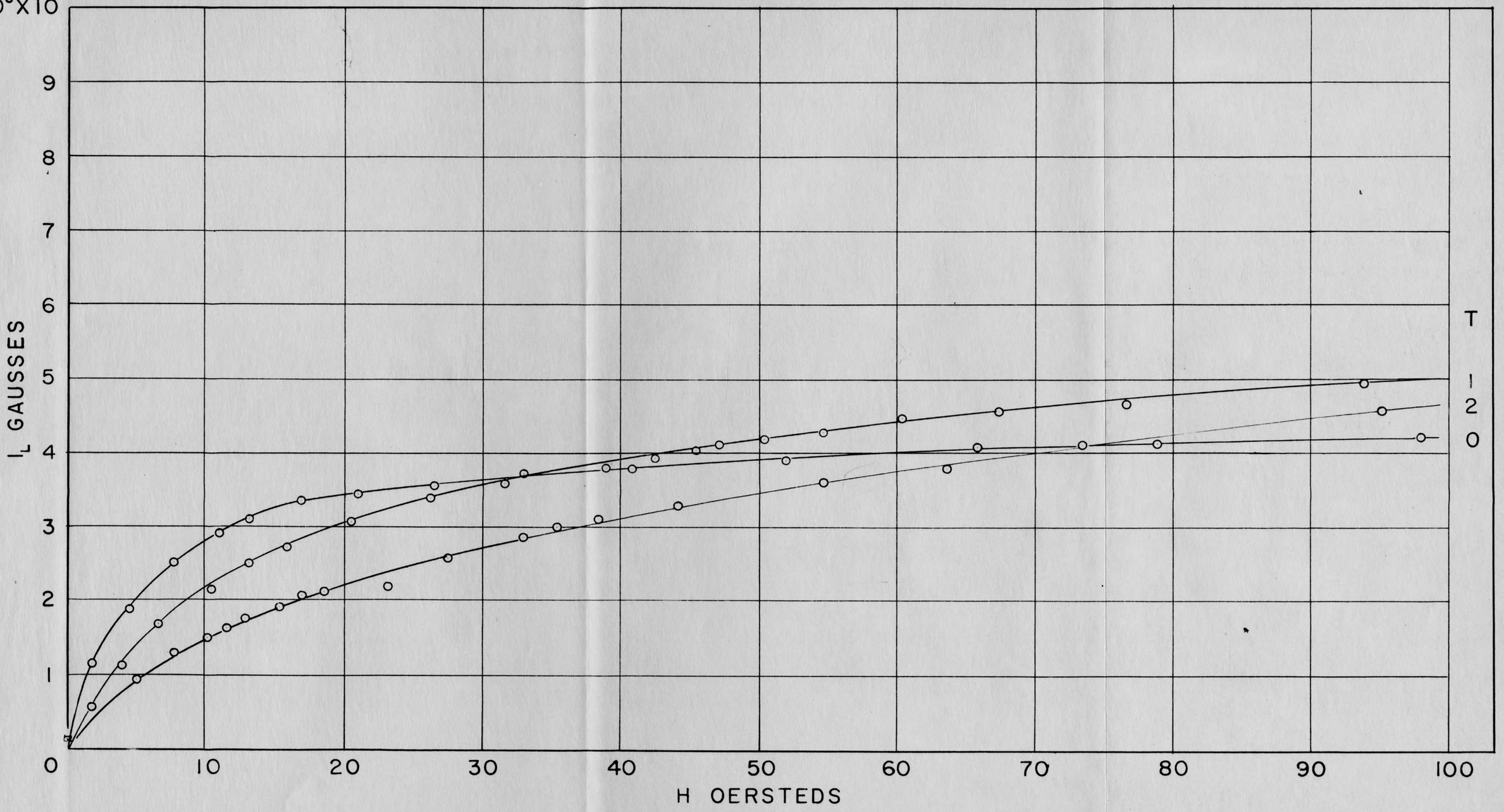
$10^3 \times 10$
9
8
7
6
5
4
3
2
1
0
I_L GAUSSES
10
20
30
40
50
60
70
80
90
100
H OERSTEDS
T
1
1
2
0

EXPLANATION OF PLATE VIII

The experimental magnetization curves for different values of angular displacement (T). One turn (T) is equal to 3.27^{o}/ cm.

Wire No. 13

Polarizing stress	0.395 kg/mm^2
Polarizing field	167 oersteds
Longitudinal stress	0.00

PLATE VIII

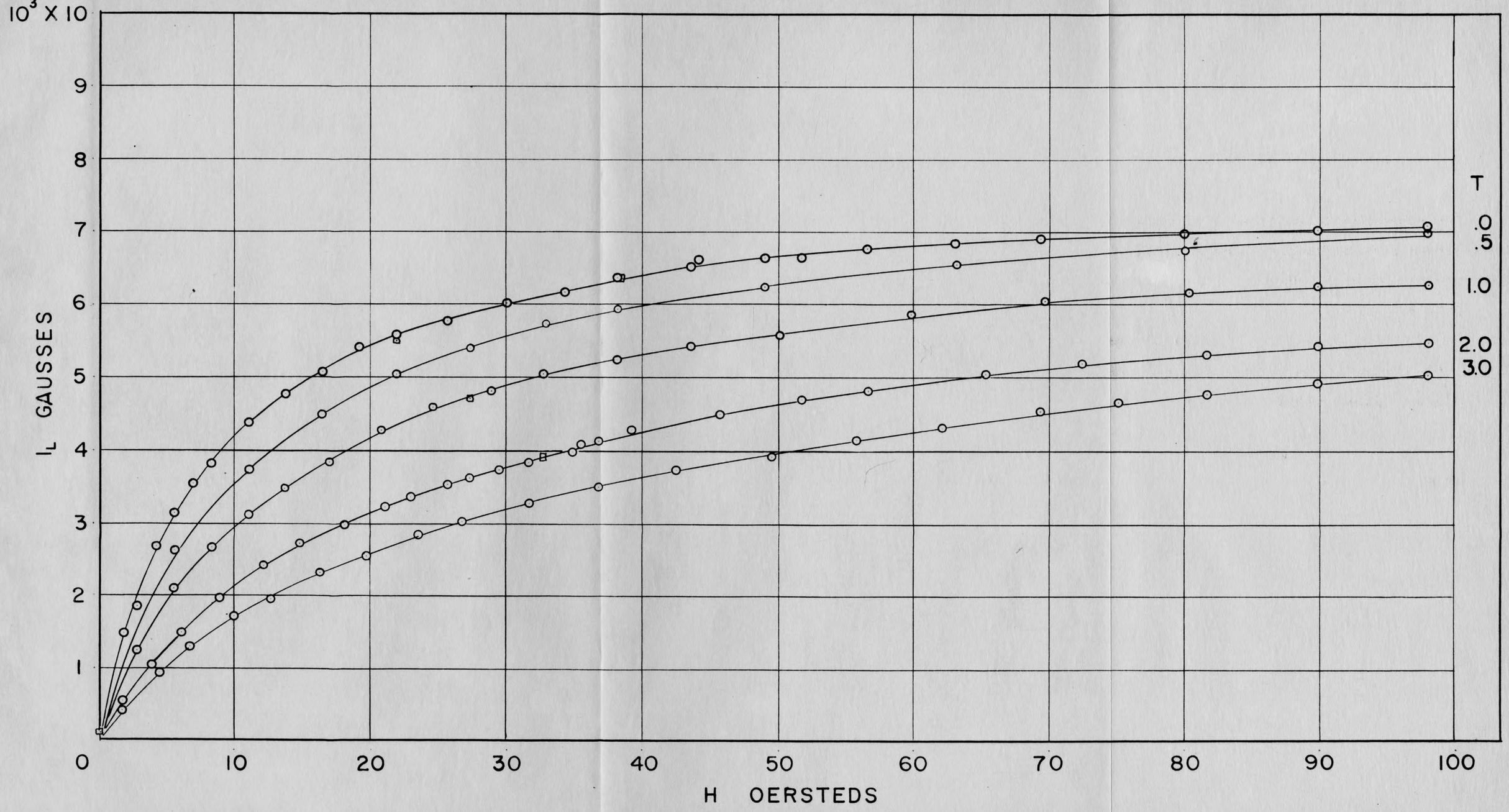
10^3 X 10
9
8
7
6
5
4
3
2
1
0
I_L GAUSSES
10
20
30
40
50
60
70
80
90
100
H OERSTEDS
T
.0
.5
1.0
2.0
3.0

EXPLANATION OF PLATE IX

The experimental magnetization curves for different values of angular displacement (T). One turn (T) is equal to 3.27°/cm.

Wire No. 9

Polarizing stress	3.95 kg/mm^2
Polarizing field	167 oersteds
Longitudinal stress	0.988 kg/mm^2

PLATE IX

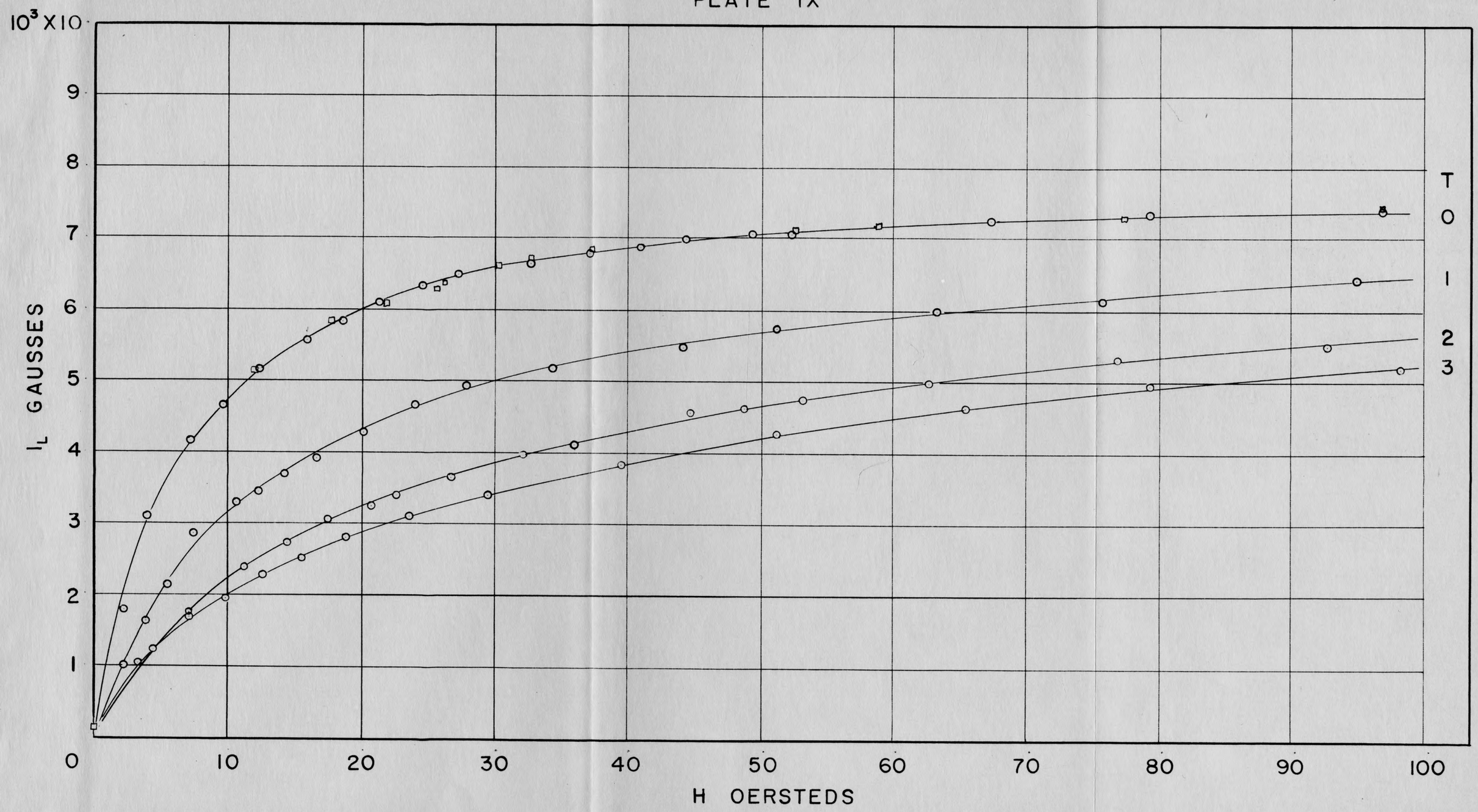
10^3 X10
9
8
7
6
5
4
3
2
1
0
I_L GAUSSES
10
20
30
40
50
60
70
80
90
100
H OERSTEDS
T
0
1
2
3

EXPLANATION OF PLATE X

The experimental magnetization curves for different values of angular displacement (T). One turn (T) equals 3.27°/cm.

Wire No. 7

Polarizing stress	5.93 kg/mm^2
Polarizing field	167 oersteds
Longitudinal stress	0.988 kg/mm^2

PLATE X

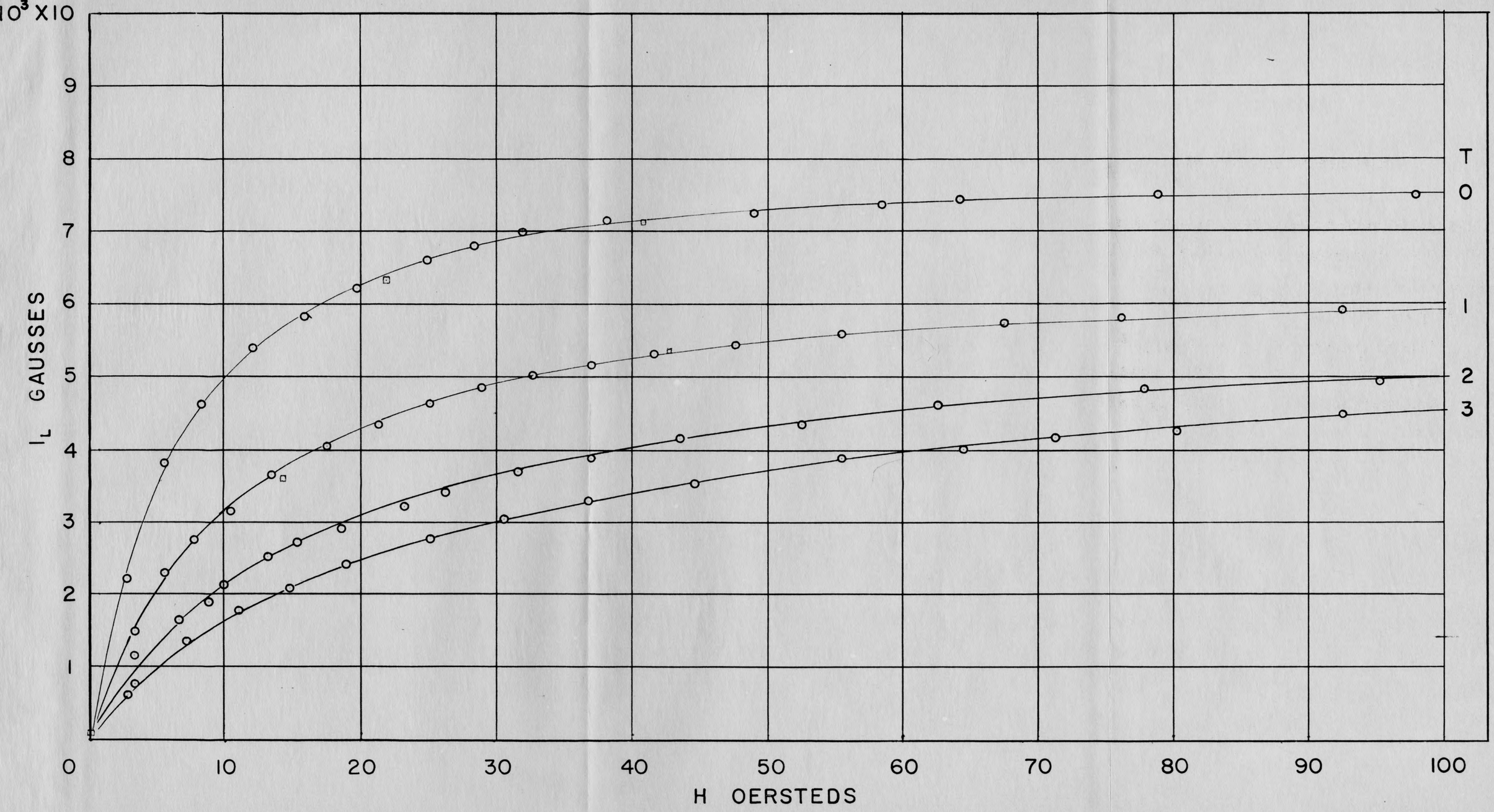
I_L GAUSSES $\times 10^3$ X10
9
8
7
6
5
4
3
2
1
0
10
20
30
40
50
60
70
80
90
100
H OERSTEDS
T
0
1
2
3

EXPLANATION OF PLATE XI

The experimental magnetization curves for different values of angular displacement (T). One turn (T) equals 3.27°/cm.

Wire No. 10

Polarizing stress	5.93 kg/mm^2
Polarizing field	167 oersteds
Longitudinal stress	0.00

PLATE XI

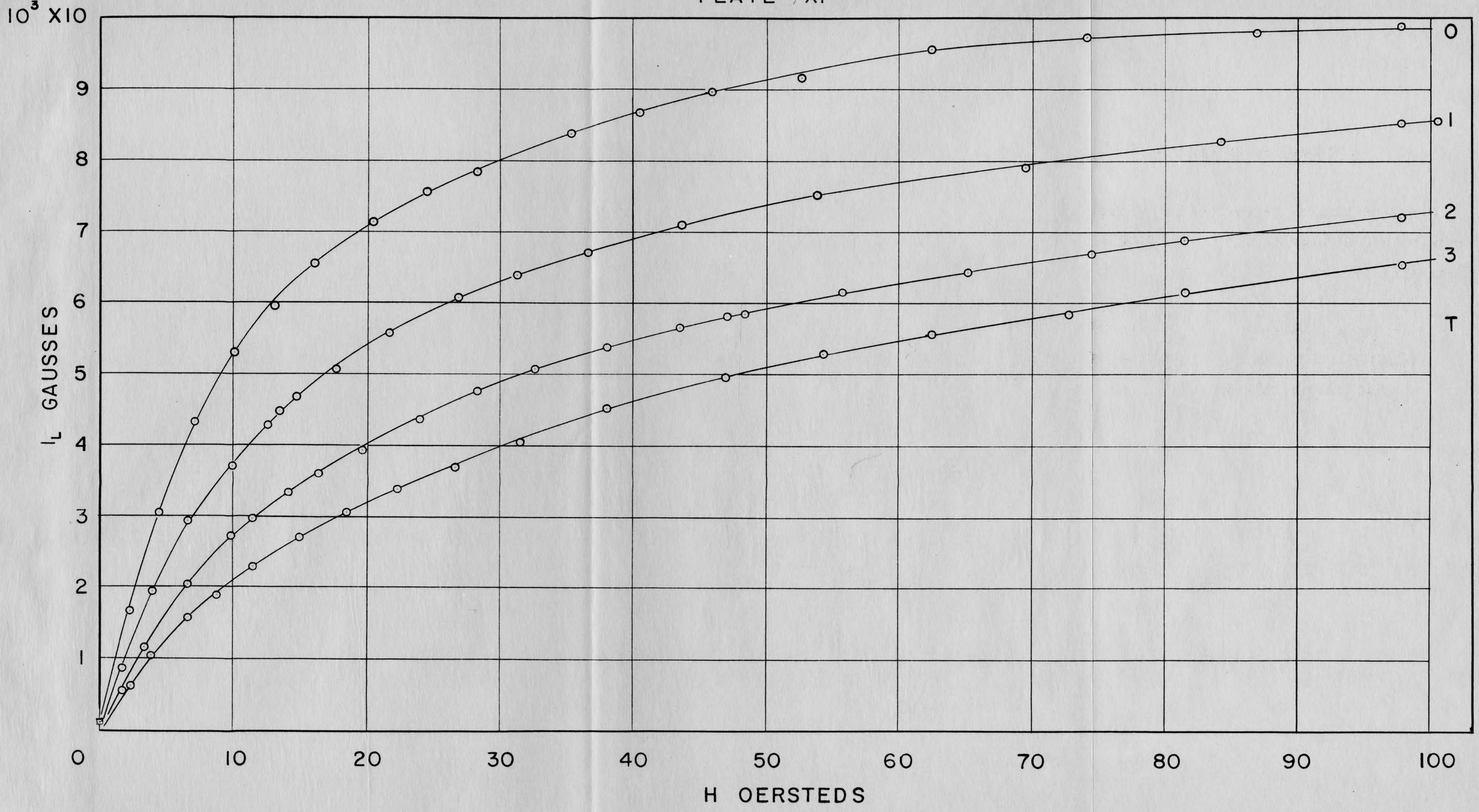
10^3 X10
9
8
7
6
5
4
3
2
1
I_L GAUSSES
0
10
20
30
40
50
60
70
80
90
100
H OERSTEDS
0
1
2
3
T

EXPLANATION OF PLATE XII

The experimental magnetization curves for different values of angular displacement (T). One turn equals 3.27°/cm.

Wire No. 11

Polarizing stress	6.92 kg/mm^2
Polarizing field	153 oersteds
Longitudinal stress	0.00

PLATE XII

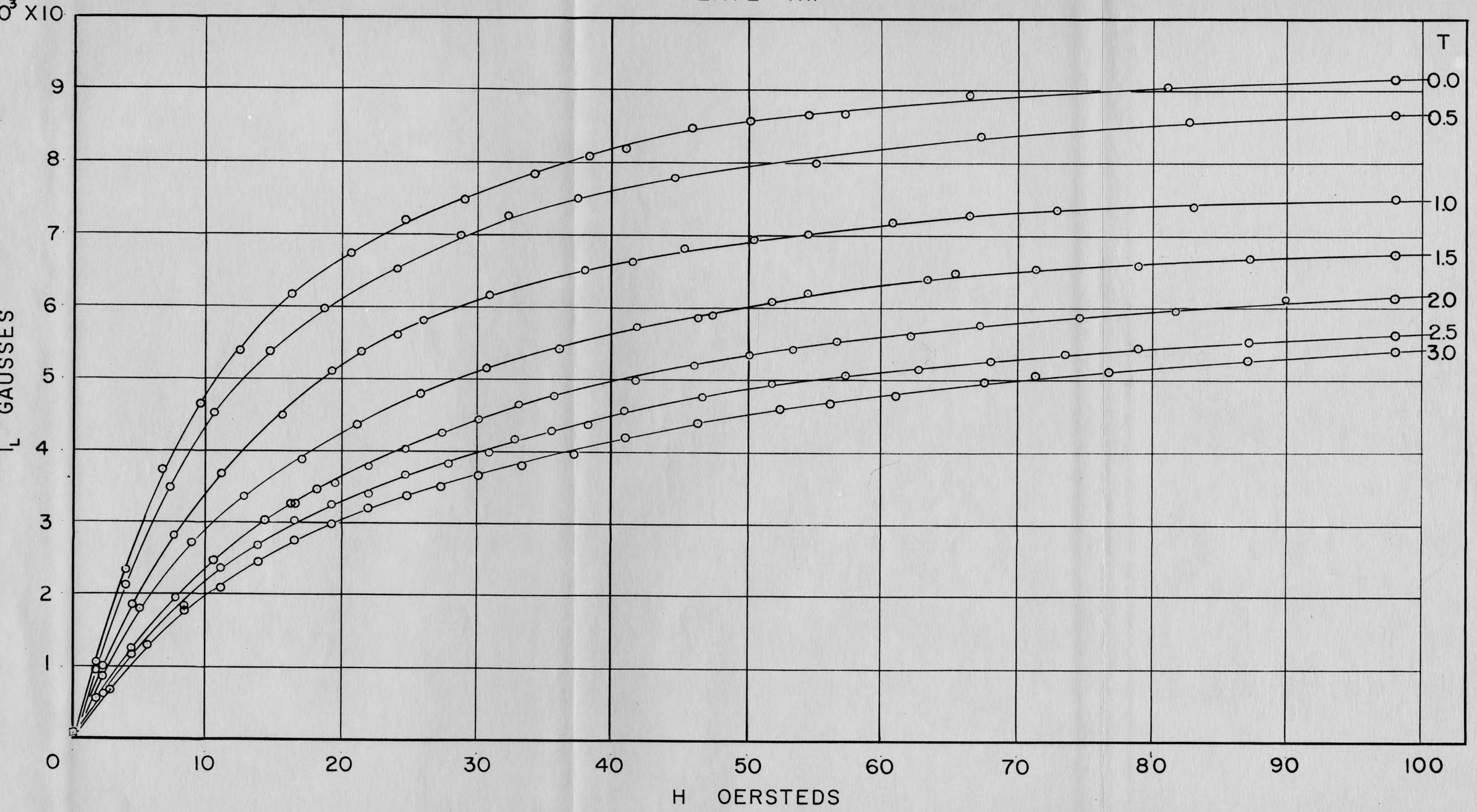
B_L^3 X10
GAUSSES
9
8
7
6
5
4
3
2
1
0
10
20
30
40
50
60
70
80
90
100
H OERSTEDS
T
0.0
0.5
1.0
1.5
2.0
2.5
3.0

EXPLANATION OF PLATE XIII

Plot of ΔI_L versus $\left(\frac{H}{d\phi/d\ell}\right)$ for data shown in Plate XI.

⊕ - 1 turn. One turn equals 3.27°/cm.

⊖ - 2 turns

○ - 3 turns

PLATE XIII

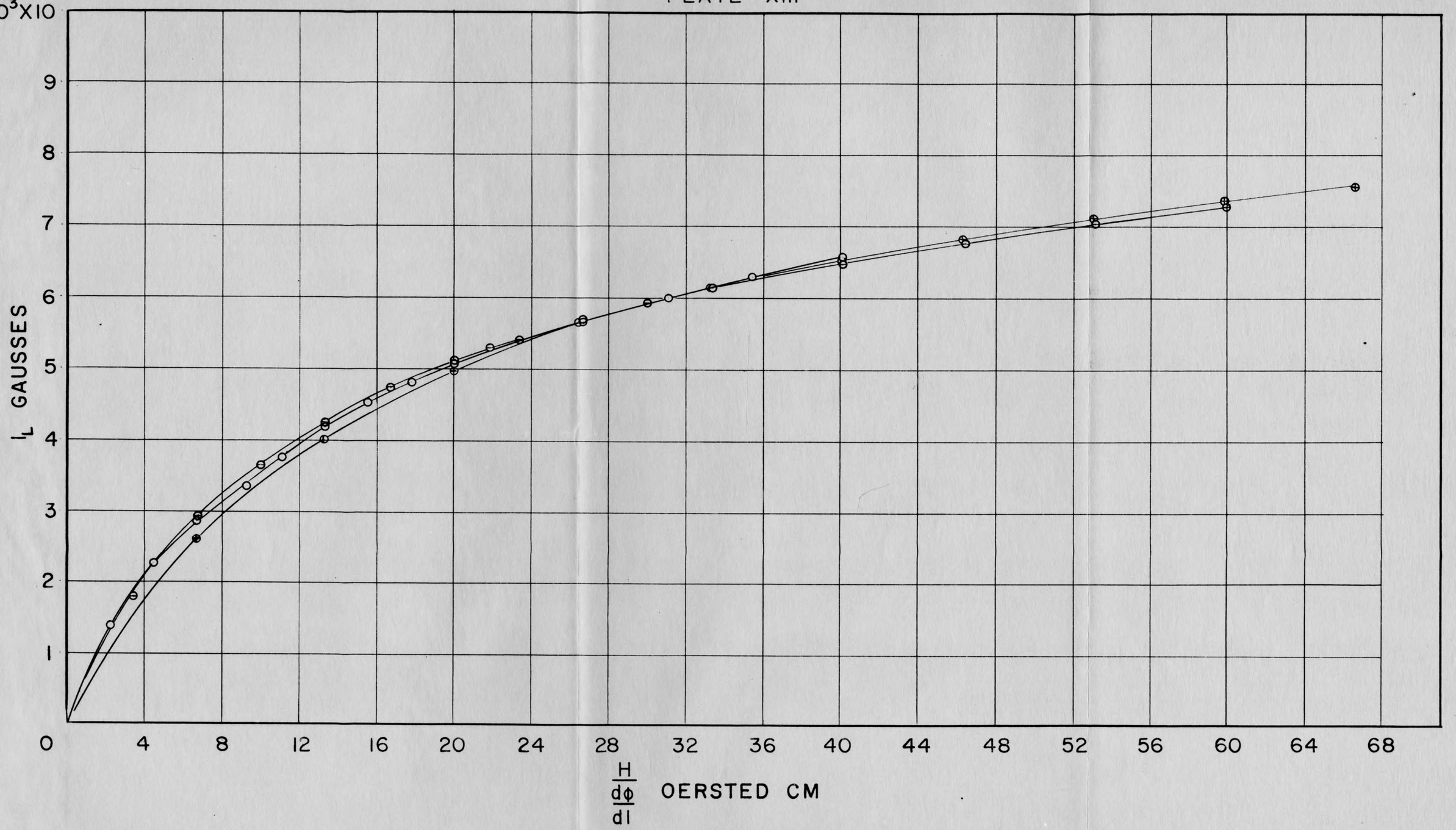
10^3X10
9
8
7
6
5
4
3
2
1
0
4
8
12
16
20
24
28
32
36
40
44
48
52
56
60
64
68
I_L GAUSSES
$\frac{H}{\frac{d\phi}{dl}}$ OERSTED CM

EXPLANATION OF PLATE XIV

Plot of ΔI_L experimental versus ΔI_L theoretical, for data shown in Plate XI. T = 1 turn = 3.27°/cm.

PLATE XIV

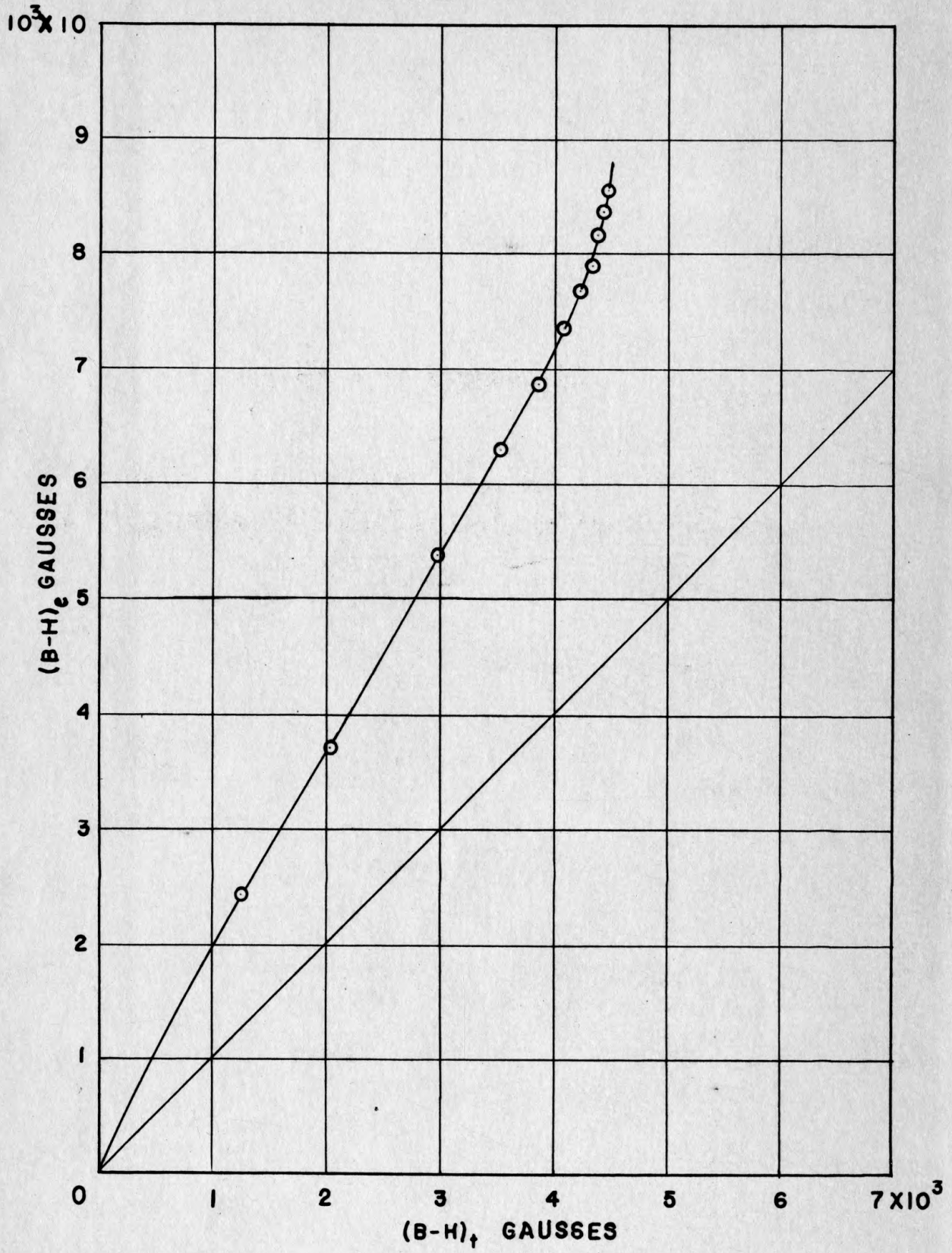
$10^3 \times 10$
9
8
7
6
5
4
3
2
1
0
$(B-H)_e$ GAUSSES
1
2
3
4
5
6
7×10^3
$(B-H)_t$ GAUSSES

EXPLANATION OF PLATE XV

Plot of ΔI_L experimental versus ΔI_L theoretical for data shown in Plate XI. T = 2 turns.

PLATE XV

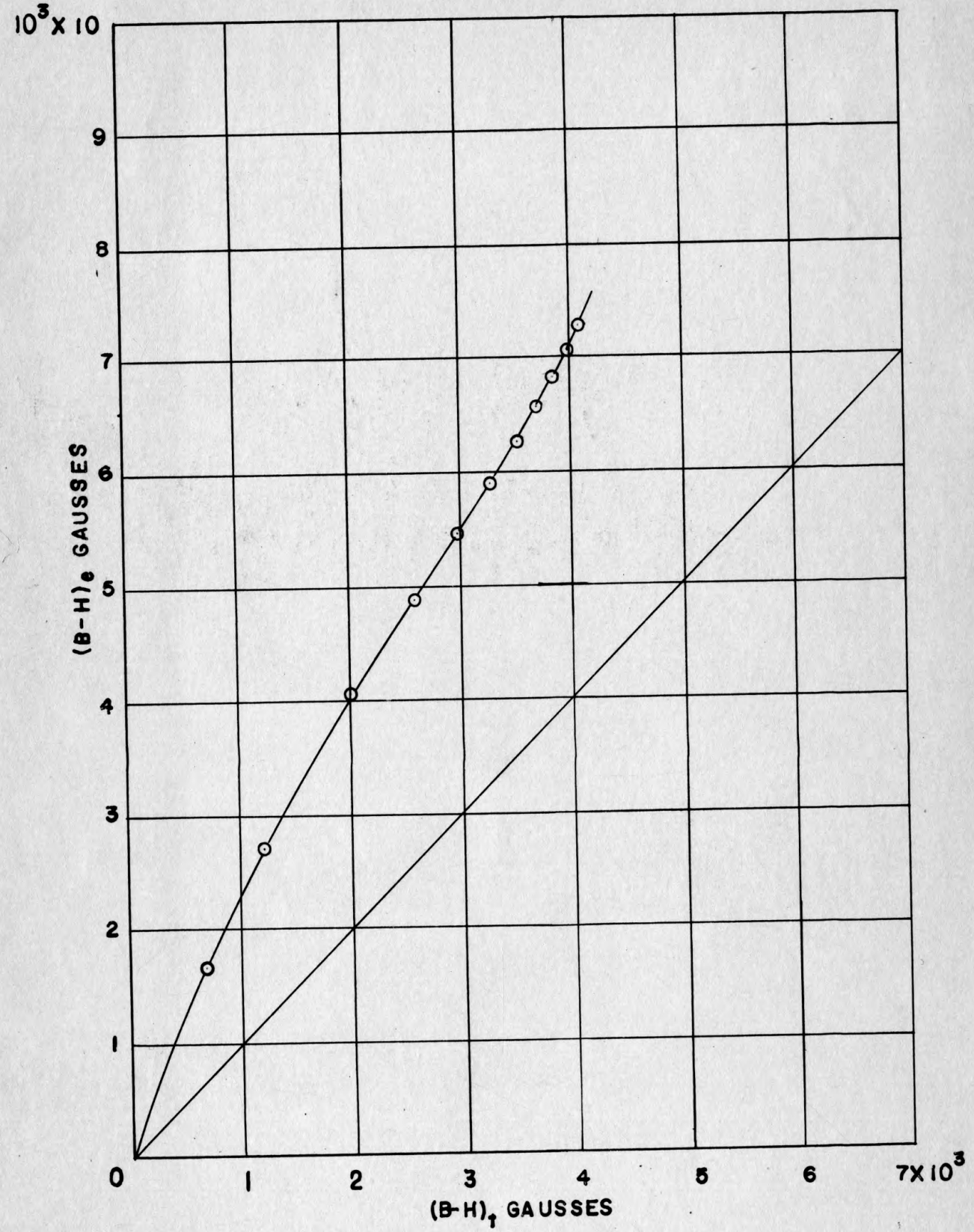

EXPLANATION OF PLATE XVI

Plot of $\triangle I_L$ experimental versus $\triangle I_L$ theoretical for data shown in Plate XI. T = 3 turns.

PLATE XVI

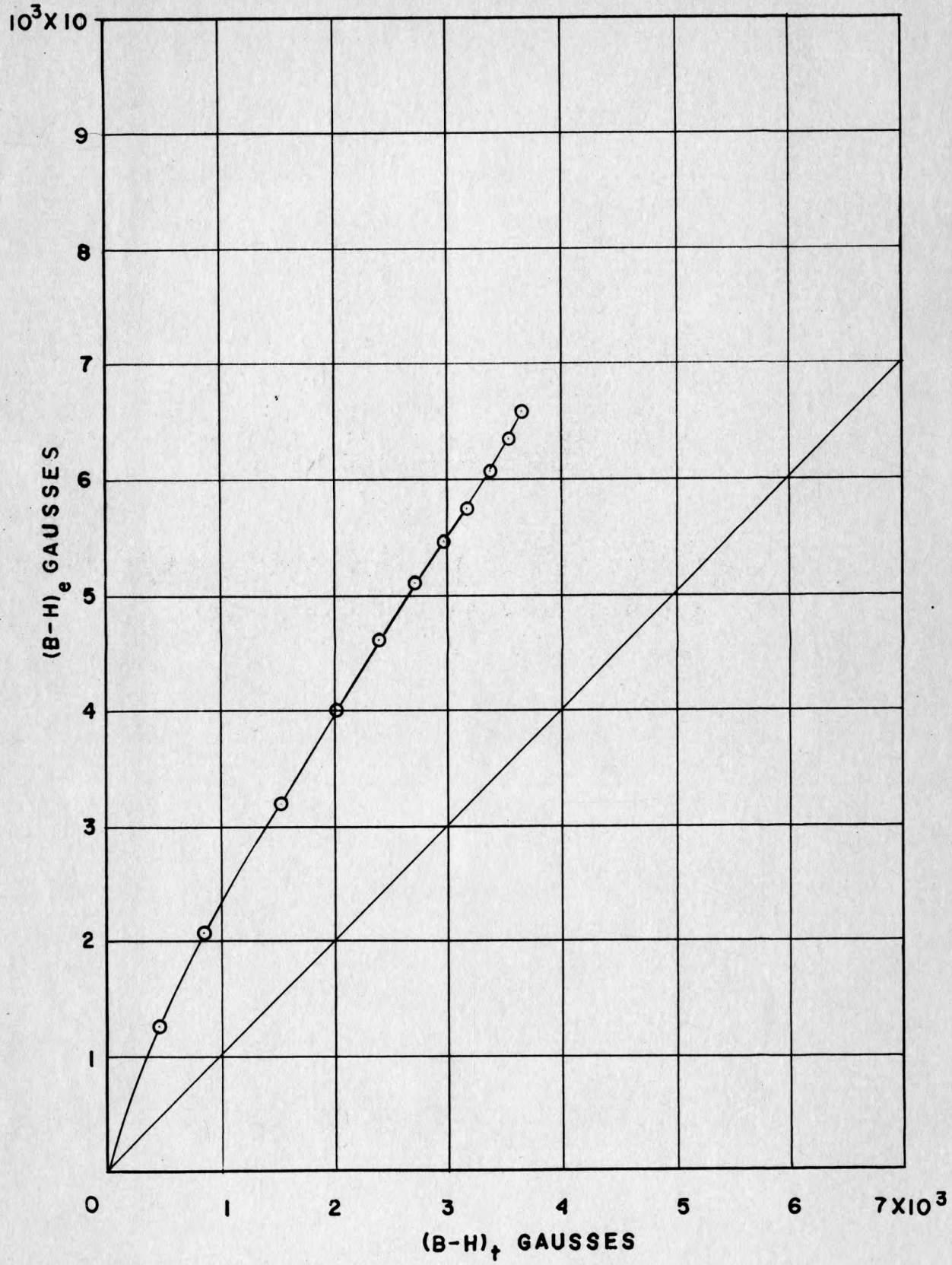

EXPLANATION OF PLATE XVII

Plot of ΔI_L experimental versus ΔI_L theoretical for data shown in Plates VII and VIII.

1. T = 1 Plate VII
2. T = 2 Plate VII
3. T = 3 Plate VII
4. T = 2 Plate VIII
5. T = 1 Plate VIII

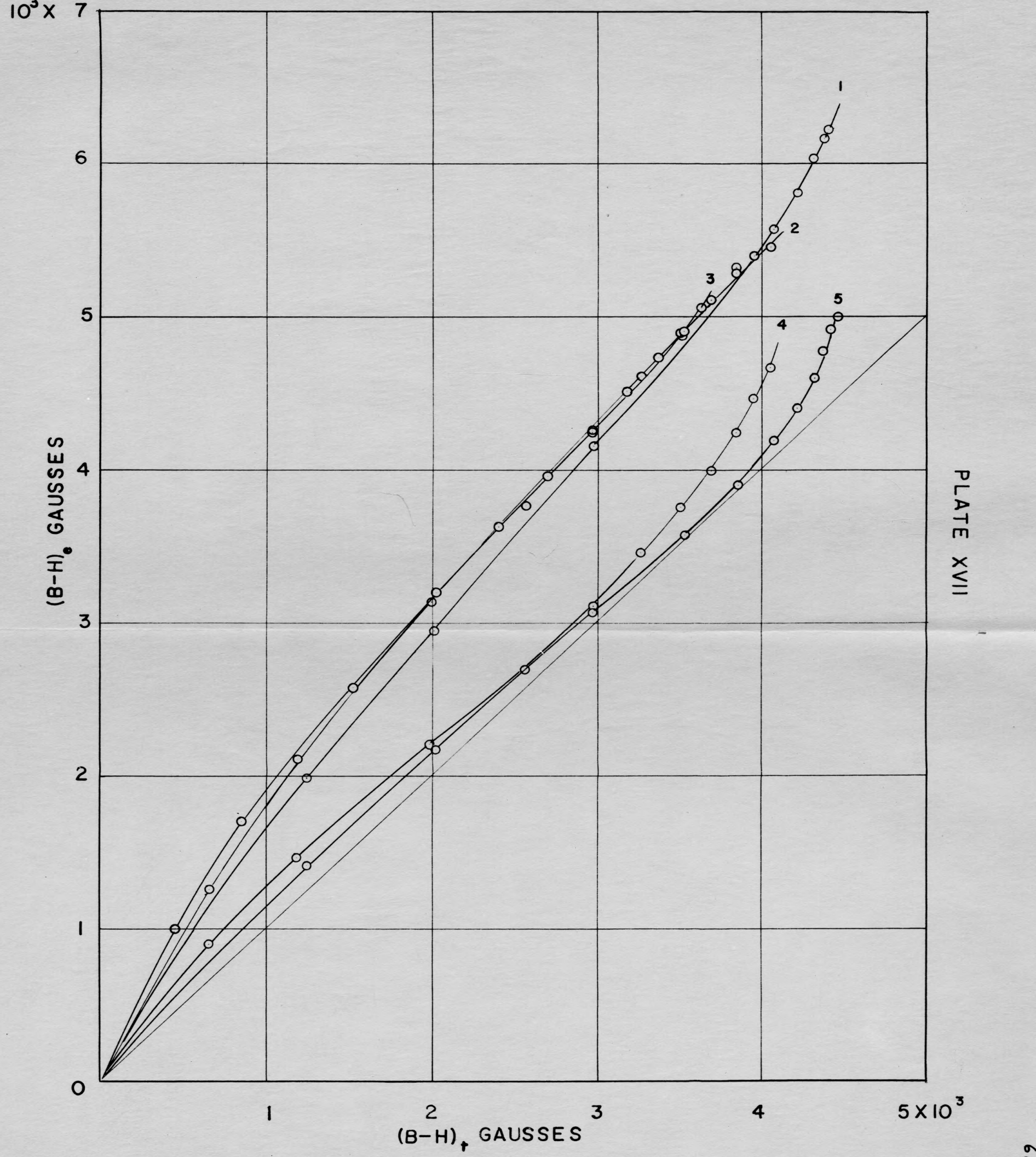

PLATE XVII

DETERMINATION OF THE LONGITUDINAL MAGNETIZATION CURVES OF POLARIZED NICKEL-IRON WIRES UNDER TORSIONAL STRESS

by

DWIGHT DANIEL BORNEMEIER

B. A., North Central College, 1956

AN ABSTRACT OF
A MASTER'S THESIS

submitted in partial fulfillment of the

requirements for the degree

MASTER OF SCIENCE

Department of Physics

KANSAS STATE UNIVERSITY
OF AGRICULTURE AND APPLIED SCIENCE

1960

Theoretical considerations by G. J. van der Maas indicate that for a polarized and torqued ferromagnetic wire the change in longitudinal magnetization $\Delta I = (I - I_r)$, (where I_r is the remanent magnetization), is a function only of $\frac{H}{d\phi/d\ell}$ (magnetic intensity divided by torque). This result was derived under the assumption that the total free energy is given by the sum of the magnetoelastic and field energies. Experimentally it is found that ΔI_L is essentially a function of $\frac{H}{d\phi/d\ell}$ for approximately the aforementioned conditions.

To approximate experimentally the theoretically assumed conditions, the samples (51 per cent Ni - 49 per cent Fe), were magnetically annealed by heating them above their curie point (510 degrees C), then cooling rapidly in a longitudinal 165-oersted magnetic field while subjected to a longitudinal stress. This treatment probably leaves some longitudinal internal stress in the wire; nevertheless the predicted relation between ΔI_L and $\frac{H}{d\phi/d\ell}$ is still found. Even when the external stress is as large as 1 kg/mm^2, ΔI_L is still a function of $\frac{H}{d\phi/d\ell}$ for small values of the applied field.

The samples were subjected to a periodic (60-cycle) unidirectional magnetic field parallel to the direction of polarization. The voltage across the search coil encircling the sample was integrated with an RC circuit which had a large time constant in comparison with the period of the applied field.